SUSPENSIONS OF CALCIUM PHOSPHATE

Interactions of milk proteins to hydroxyapatite

Ying Chen

Supervisors: Lilia Ahrné, Kristian Raaby Poulsen, Colin Ray, Frida Lewerentz
Examiner: Marie Paulsson

Department of Food Technology, Engineering and Nutrition

Lund University, 2022

Abstract

Capolac is a product containing hydroxyapatite (HA) from Arla Food Ingredients, to be used for calcium fortification. The adsorption of casein and whey proteins onto the Capolac was investigated, aiming to solve the sedimentation problem of this insoluble calcium phosphate.

The adsorption of casein from sodium caseinate (SC) and whey protein from whey protein isolate (WPI) was first analyzed with pure HA particles. Different particle size of HA was explored. Zeta-potential measurements and the suspension behavior observations showed that both casein and whey protein adsorbed onto HA particles. The smaller the particle size, the better the suspension stability.

Then the adsorption of SC and WPI onto Capolac was explored. Results of zeta-potential measurements, SDS-PAGE, surface protein coverage calculation and turbidity measurements suggested both SC and WPI bound to Capolac and improved the suspension stability. Data analysis was performed to compare the protein adsorption to HA and Capolac, results showed that there was no significant difference between the two particles, means the casein and whey protein adsorb onto both HA and Capolac particles. The higher absolute value of zeta-potential for pure Capolac than pure HA, and the turbidity measurement of pure Capolac indicate a better suspension stability for pure Capolac than pure HA particles. Possible reasons behind this are discussed, in relation to the produce process of Capolac.

The adsorption of SC and WPI on to both particles could be fitted in a simple Langmuir model, demonstrating a single layer adsorption of both proteins to the surface of the HA and Capolac particles.

Findings from this study proved that both SC and WPI-coated Capolac particles improved the suspension stability. However, the adsorption is a complicated process, the stability and application of the coated particles requires further investigation.

Acknowledgement

This degree project in Faculty of Engineering, Lund University is cooperated and supported by Department of Food Science in University of Copenhagen and Arla Food Ingredients. I'm happy that I made this far with people involved and being supportive.

First, I would like to express my sincere appreciation to my main supervisor, Prof. Lilia Ahrné. Thanks for providing the expert assistance, support, advice, and encouragement though out the entire project.

I would also like to give my great thanks to my other supervisors Frida Lewerentz, Kristian Raaby Poulsen and Colin Ray. I am very grateful to their guidance and extensive help on the research activities and scientific writing skills.

Thanks to my examiner Marie Paulsson, for her kindness and valuable input on the report and thesis presentation.

Special thanks to my family, who always trust in me and give me unlimited support along the journey.

Last but not least, many thanks to everyone that is involved, and I have been working alongside through the project.

Table of contents

1. Introduction

Calcium is one of the essential minerals for the human body, functioning in the formation of bone and teeth, muscle contraction, blood clotting, normal cardiovascular function and maintaining the function of many enzymes. As a vital element for skeleton health, about 99% of the body's calcium is stored in the bones and teeth, in which the reservoir provides support for both intra- and extracellular calcium. Lack of calcium intake leads to osteoporosis. Thus, adequate intake of calcium can not only reduce the risk of bone loss but also prevent many diseases such as hypertensive disorders, coronary artery, etc. (Palacios et al., 2021).

Dietary sources are the best way to obtain sufficient calcium, for example, dairy products. As a naturally rich calcium source, dairy products are well-known for bone health, as a result, calcium fortification in dairy products would be highly acceptable to consumers (Tercinier, 2016). However, it is challenging to meet the recommended calcium requirement in the absence of dairy products. Thereby calcium fortification in foods emerges for the reasons stated above, which offers individuals a crucial way to increase their calcium consumption.

Among common calcium fortification sources in dairy products, calcium phosphate is an inorganic calcium salt with high calcium content but relatively lower solubility. It is widely applied in industries as a nutrient supplement. Hydroxyapatite, as a highly crystalline formality of calcium phosphate, is a popular source of tricalcium phosphate applied in these products.

Capolac, developed by Arla Food Ingredients, is high in calcium content and contains 70% of hydroxyapatite (de Zawadzki & Skibsted, 2019), can be applied in a wide range of food and beverage systems to achieve the fortifying effect. This is a natural milk mineral concentrate derived from milk with a similar chemical composition to human bone and teeth (Arla product sheet, see *Appendix 1*).

While the calcium fortification products look more nutritionally attractive to consumers, the development of these products has run across more than a few roadblocks because calcium may react with protein particularly when heat treated, causing problems like sedimentation, and gelation, depending on the type of calcium salts added. Certain stabilizers and emulsifiers have been implemented in these products to retain the calcium in suspension in order to upgrade mouthfeel and appearance (Singh et al., 2007). Unfortunately, issues like low soluble calcium concentrations, suspension settlement issues, undesirable off-flavors such as bitter, metallic, chalky, or mineral-like, poor textures due to added stabilizers or chelating agents, or a combination of these downsides appear when developing calcium-fortified products (Singh et al., 2007).

Aim and scope

The goal of this project is to seek a way to coat Capolac to improve the suspension stability, therefore addressing the difficulties listed above.

A research project conducted by Tercinier et al. (2012) found that sodium caseinate (SC) and whey protein isolate (WPI) adsorbed on hydroxyapatite (HA) particles, thus improving the suspension stability of the particles. As Capolac is a product mainly contains hydroxyapatite, this study is aiming to measure the adsorption of sodium caseinate (SC) and whey protein isolate (WPI) to this product, as well as to investigate if the coated Capolac particles can increase suspension stability.

This work will first be conducted on pure hydroxyapatite particles to verify if milk proteins (SC and WPI) adsorb on them, then test the product Capolac to examine the protein adsorption and suspension ability of the coated particles.

2. Theoretical background

2.1. Calcium fortification in food

2.1.1. The role of calcium and deficiency problems

Nowadays, the nutritional significance of calcium is receiving more attention because many people, especially women and adolescents do not take their recommended dietary allowance of calcium, and the calcium shortage leads to the development of osteoporosis and other illnesses (Mehta, 2022; Pawal, 2019). Milk products contribute significantly to calcium and phosphorus intake. It is speculated that calcium phosphate is a more favorable form that has a long-term effect on human bone health (Cashman, 2006).

Calcium deficiency is the most common and prevalent mineral deficiency problem. The human body weight contains approximately 2% of calcium, and 99% of calcium is present as a multiple apatite salt, including calcium phosphate in the skeleton and teeth (Lancker, 1976). Besides being stored in the bone, calcium also contributes to nerve tissue's normal function and muscle contraction. It plays a vital role in myocardial function and is essential for enzymes performing in all biological systems (Tunick, 1987).

Over the past few years, some diseases such as osteoporosis, hypertension, colorectal cancer, and amyotrophic lateral sclerosis have been detected to be related to calcium shortage and low ratios of calcium to phosphorus. Thus, the role of calcium in the human body has raised a good deal of public attraction. However, approximately 70% - 80% of calcium will be excreted as feces which means the human body only adsorbs 30% of the total calcium from food digestion, making it more challenging to meet the recommended daily calcium intake (Fardet et al., 2019). Vitamin D plays a significant role in calcium absorption, which could be obtained from the synthesizing in the skin upon exposure to ultraviolet light and some food with fortified vitamin D. Still, there are numerous factors that could hinder calcium absorption, such as oxalic acid or phytic acid found in cocoa, spinach or cereals, etc. to form insoluble salts with free calcium, the ratio to phosphorous, alcoholism, lack of physical activity, stress, illness and so on (Palacios et al., 2021; Theobald, 2005; Tunick, 1987; Weaver, 1998).

There is no universal criterion for defining calcium recommendations worldwide due to different methodologies, nomenclatures, age groups, and the intake of phytate, salt, and vitamin D for diverse populations. Table 1 shows the calcium recommendations depending on age, gender, and life stages from World Health Organization (WHO)/Food and Agriculture Organization (FAO) (Joint, 2004; Organization, 2004).

Table 1. WHO/FAO recommended calcium allowances based on Western European, American and Canadian data (Joint, 2004; Organization, 2004).

Group	Calcium intake mg/day
Infants and children	
0-6 months	
Human milk	300
Cow milk	400

7-12 months	400
1-3 years	500
4-6 years	600
7-9 years	700
Adolescents, 10-18 years	1300
Adults	
Females	
19 years to menopause	1000
postmenopause	1300
Males	
19-65 years	1000
65+	1300
Pregnancy (last trimester)	1200
Lactation	1000

In the United States and some European countries, country-specific recommendations are higher than that from WHO. According to the Food and Nutrition Board (FNB) in the United States, the Recommended Dietary Allowance (RDA) for healthy adults and children is 800 mg/d, and for pregnant women and teenagers (10-18 years old) is up to 1300 mg/d (Ross, 2011). With the progress of research and concerning of osteoporosis, the RDA has been proposed by the National Institutes of Health to increase to 1000 to 1500 mg per day. Under this circumstance, the average intake of calcium is below the RDA for most people, from teenagers to the mid-aged group, especially for women; three-quarters of women over age 35 consume less calcium according to their RDA. Calcium has been one of the three nutrients consumed below the RDA for Americans for over 30 years (Clark, 1958).

In other countries, calcium intake differs widely worldwide between groups and populations. The variations are high in all age groups, from children to the elderly in different countries. For example, girls aged 5-12 years consume calcium from as low as 234 mg/day in Indonesia to as high as 1151 mg/day in Canada (Palacios et al., 2021). Typically, the low consumption of calcium is seen in low- or middle-income countries like Argentina, Brazil, Malaysia, Philippines. Asian countries have inadequate intakes of dairy products traditionally; take China, for example, the primary calcium sources are vegetables, legumes, and cereals (Huang et al., 2018). For pregnant women, if considering a threshold of 800 mg/day, 28% of high-income countries reported low intake, while this number is up to 88% in low- and middle-income countries (Cormick et al., 2019).

2.1.2. Different calcium sources and their applications

Plenty of food sources contain a significant amount of calcium, such as tofu, broccoli, some seafood, dark green leafy vegetables like curly kale, okra, collard, and leading sources - dairy products. Dairy products are the most favorable calcium sources not only because of the high amount of calcium and the good absorptivity in the human body but also the frequency of consumption by most people (Tunick, 1987). Thus, as a response to the increased publicity of this mineral, dairy processors have started to address this issue and mark their products with a high calcium content. One can reach their calcium RDA by only drinking one glass of milk if it is fortified with tricalcium phosphate.

However, in the absence of dairy products, the recommended nutrient requirements are difficult to meet for a large portion of people worldwide, especially for the low-income population.

Calcium fortification emerge as a way to improve calcium intake and reduce health risks caused by calcium deficiency, especially for pregnant women. Calcium supplementation in pregnant women can reduce the risk of preeclampsia for both mother and infant, which is a life-threatening condition. Direct consumption of calcium supplements has limitations such as high cost, pill burden, side effects, and possible excessive calcium intake (>2500 mg/day), etc. Hence, the focus has moved to a more effective and economical way of calcium fortification in foods, particularly in staple foods. Palacios et al. have reported that calcium-fortified wheat flour has contributed 13-14% of calcium intake for British people. If this mineral were removed from the wheat flour, approximately 21% of girls, 12% of boys, and 6-9% of women aged 19-64 years would have a lower intake than the reference (Palacios et al., 2021).

Micronutrient fortification programs have been widely implemented globally. The most common nutrients added are iodine, iron, folic acid, vitamin A, etc. Yet calcium is less frequently added. By far, the UK is the only country that mandatory calcium-fortified in staple food wheat flour (Palacios et al., 2021). Other popular food sources currently calcium-fortified have dairy products, fruit juices, snacks, breakfast cereals, sports and energy beverages, infant formulas, and egg products. Different programs and regulations apply and are customized in different regions.

Calcium salts like calcium carbonate, calcium gluconate, and calcium lactate are the leading agent that is added to fortified foods. Inorganic calcium salts are more economical with high calcium content, while organic calcium salts have higher bioavailability. Calcium chloride, calcium gluconate, and calcium lactate have been studied, and the addition is likely to reduce pH and increase ionic calcium, shifting the heat coagulation-pH profile in a more alkaline direction, as a result of poor heat stability (Omoarukhe et al., 2010). Calcium carbonate is proved to be an effective supplementation because of its insolubility, but its properties have not been thoroughly investigated (Singh et al., 2007).

Similar to the bone mineral composition, calcium phosphate is of higher interest as a calcium supplement because of its insolubility; it will not change the pH or ionic calcium or alter buffering capacity (Lewis, 2011). On the other hand, low solubility may damage mouthfeel, mainly related to chalkiness and grittiness, and the suspension stability needs to be further explored, which is also the aim of this study.

There are quite a few forms of known calcium phosphates, including monocalcium phosphate monohydrate (MCPM), monocalcium phosphate anhydrous (MCPA), amorphous calcium phosphate (ACP), α-tricalcium phosphate (α-TCP), β-tricalcium phosphate (β-TCP), hydroxyapatite (HA) and so forth (Amjad, 2013). Dicalcium and tricalcium phosphates increase calcium balance in elderly patients because they are soluble in digestive juices.

2.2. Composition and structure of milk

Milk is a nutrient-rich liquid secreted from the mammary glands of mammals such as cows, buffaloes, goats, sheep, etc. Humans have consumed them for a long time because of their richness in nutrients. Cow milk is the most widely consumed type among all mammals, which mainly constitutes water, milk solids like protein, fats, carbohydrates, and a variety of vitamins and minerals. Table 2 demonstrates the main components of “normal milk” (referred to as cow’s milk here unless otherwise stated).

Table 2. The main composition of milk (McKenzie, 1967; Walstra et al., 2005).

Component	Average Content in Milk (% w/w)	Range (% w/w)
Water	87.1	85.3-88.7
Solids-not-fat	8.9	7.9-10.0
Fat in dry matter	31	22-38
Lactose	4.6	3.8-5.3
Fat	4.0	2.5-5.5
Proteins	3.3	2.3-4.4
Caseins	2.6	1.7-3.5
Mineral substances	0.7	0.57-0.83
Calcium	0.13	-
Magnesium	0.01	-
Organic acids	0.17	0.12-0.21
Miscellaneous	0.15	-

As seen in table 2, milk is rich in protein and calcium which serve as a major calcium and protein dietary source for humans. The main objective of this project is to investigate the interaction of milk protein with hydroxyapatite - a source of calcium fortification, so the main focus of this section on milk composition is primarily on protein and minerals. The source of milk protein in this study is whey protein isolate and sodium caseinate, which will be addressed in a later section (*Section 2.3*).

2.2.1. Milk proteins

Normal bovine milk protein concentration is approximately 3.5% (Fox et al., 1998). Milk protein is a complicated system from which the individual components are hard to separate because some of the proteins are very closely related. Table 3 presents an overview of milk proteins.

Table 3. Overview of proteins in the milk (Walstra et al., 2005).

Protein	mmol/m^3 Milk	g/kg Milk	g/100 g Protein
Casein	1120	26	78.3
α_{s1}-Casein	450	10.7	32
α_{s2}-Casein	110	2.8	8.4
β-Casein	360	8.6	26
κ-Casein	160	3.1	9.3
γ-Casein	40	0.8	2.4
Serum Proteins	~320	6.3	19
β-Lactoglobulin	180	3.2	9.8
α-Lactalbumin	90	1.2	3,7
Serum albumin	6	0.4	1.2
Protease peptone	~40	0.8	2.4
Immunoglobulins	~4	0.8	2.4
Miscellaneous		0.9	2.7
Lactoferrin	~1	0.1	-
Transferrin	~1	0.01	-
Membrane proteins	-	0.7	2
Enzymes	-	-	-

According to table 3, milk proteins are separated mainly into two groups, casein, and serum proteins, each containing several different proteins. Casein, as the principal protein group of

milk, is a mixture of several components always presenting as large aggregates in milk which are called casein micelles. The casein micelles contain about 94% protein and 6% low molecular mass, colloidal calcium phosphate (CCP) which dissolves on acidification (Fox et al., 1998). Casein micelles usually are in spherical shape and quite tightly packed. The large surface area of the micelles is significant for its behavior; for example, the white color of the milk is primarily due to the light scattering by casein micelles.

The stability and behavior of the micelles are critical to many dairy processing operations such as cheese manufacture, frozen products, and so on. There are several proposed models of micelles, with some common points like core-coat structure, submicelles, and CCP as an integrating factor. No matter what model it has, caseins have functions to enable a high concentration of calcium to be carried in a stable form in milk.

Caseins are hydrophobic, and with a relatively high charge, the molecules can hardly be denatured because of the little secondary and tertiary structure. There are several different caseins in milk, and they are hardly separated under precipitation from milk. A commonly used method -electrophoresis could be feasible to separate caseins after dissolving the casein micelles with a reducing agent. α_{s1}, α_{s2}, β and κ are the four distinct peptide chains of casein. α_{s1}-casein has a high phosphate content and a high net negative charge, α_{s2}-caseins are rather Ca^{2+} sensitive, β-casein is the most hydrophobic one with unevenly distributed charge. κ-casein differs significantly from the other caseins. It occurs in milk as oligomers because of the intermolecular disulfide bonds formed by cysteine residues. The "hairs" of κ-casein, which is the hydrophilic Carboxyl (C)-terminal part sticking out from the micelle core, are crucial in providing the stability of the micelles against the flocculation (Walstra et al., 2005) (Tuinier & De Kruif, 2002; Walstra, 1990).

From a nutritional perspective, casein is capable of binding large amounts of important nutrients like calcium and phosphate, in such a way as to provide essential minerals for bones.

Serum proteins normally called whey proteins, are present as a dissolved form in the serum, which makes up around 20% of the total protein in the bovine milk (Fox et al., 1998). Most of the whey proteins are globular with a relatively homogeneous charge distribution. The main components of whey protein are β-lactoglobulin (~50-55%), α-lactalbumin (~20-25%), proteose peptone (~10-15%), immunoglobulins (~1%), serum albumin (~2%) (Hulmi et al., 2010; Walstra et al., 2005). α-lactalbumin is a small, compactly folded, roughly spherical molecule with a specific nonexposed binding site for a calcium ion (Walstra et al., 2005). β-lactoglobulin is the major serum protein that almost dominates the whey protein properties. With changes in pH or temperature, this protein's tertiary and quaternary structure undergoes a number of alterations, see figure 1. β-lactoglobulin has the ability to bind many hydrophobic molecules, and it is the carrier for retinol.

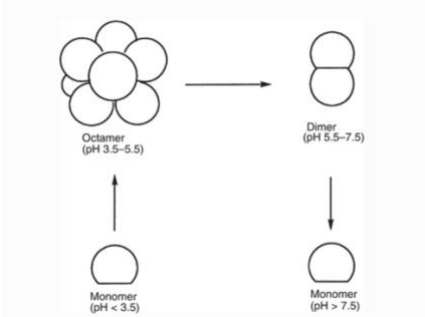

Figure 1. Effect of pH on the quaternary structure of β-lactoglobulin (Fox et al., 1998).

From a nutritional perspective, whey protein is a high-quality protein containing plenty of essential amino acids required to stimulate protein synthesis and support muscle building (Hulmi et al., 2010). The high and fast rate of amino acid availability makes whey protein especially important for athletes and around workouts, and the superiority of whey over soy or casein at stimulating muscle protein synthesis (Hulmi et al., 2010). Whey protein also has an anticancer, and antimicrobial effect and could serve as a potent growth stimulant for a certain number of mammalian cells (Smithers et al., 1996).

Other serum proteins like serum albumin and immunoglobulins have a small proportion in milk and would not be able to detect through this research; thus, they will not be addressed in this section.

2.2.2. Minerals

Besides proteins and other components like fat, lactose, vitamins, and minerals are also vital in milk. It contains cations – calcium, magnesium, sodium, and potassium, as well as anions – inorganic phosphate, citrate, and chloride (Gaucheron, 2005). These inorganic and organic ions of milk interact with both casein and nonmicellar proteins; thus, understanding the theoretical background of milk minerals is of great importance to solving dairy processing problems and understanding fundamental research. Table 4 indicates the composition of milk minerals.

Table 4. Mineral composition of cow milk (Gaucheron, 2005; Walstra et al., 2005).

Compound	Range (mmol/kg)	Average (mg/kg)
Cations		
Sodium (Na)	17-28	480
Potassium (K)	31-43	1430
Calcium (Ca)	26-32	1170
Magnesium (Mg)	4-6	110
Amines	~1.3	-
Anions		
Chloride (Cl)	22-34	1100
Carbonate (CO_3)	~2	100
Sulfate (SO_4)	~1	100
Phosphate (PO_4)	19-23	2030
Citrate	7-11	1750
Carboxylic acids	1-4	-
Phosphoric esters	2-4	-

All of these elements are distributed differently in the milk. The milk ions can exist in the form of hydrated ions or bound to proteins in the serum or caseins in the micelles, or bound to other

ions. Magnesium, calcium, and inorganic phosphate are partially bound to the casein micelles, while other non-binding ions, potassium, sodium, and chloride are essentially diffusible. The aqueous milk phase contains around one-third of calcium, half the inorganic phosphate, two-thirds of magnesium, and over 90% of citrate (Gaucheron, 2005).

Phosphate has been generally accepted as the ion bound to calcium to form calcium phosphate. Part of the salts in milk in present on casein micelles as colloidal calcium phosphate, which also includes other components, i.e., potassium (K), Sodium (Na), Magnesium (Mg), and citrate. This micellar calcium phosphate is mainly associated with α_{s1}-, α_{s2}-, β-caseins, contributing to the structure and stability of casein micelles. However, the composition and structure of casein micelles may be affected under small changes of physicochemical conditions, such as acidification, heat treatment, cooling, etc. (Walstra et al., 2005).

From the nutritional perspective, there are 20 essential minerals for human beings, including macrominerals such as sodium, potassium, chloride, calcium, magnesium, phosphorus, and trace elements like iron, copper, zinc, manganese, selenium, iodine, chromium, etc., which are all moderately present in milk (Cashman, 2006). Calcium is the most associable milk mineral related to bone health of the 20 essential minerals, a more detailed description could be seen in *section 2.1 Calcium fortification in food*.

Phosphorus is another essential nutrient in milk, and the ratio to calcium is pivotal to human bone health. It has proved that excessive phosphorus might influence bone health, especially when calcium intake is low. Because the increased serum phosphorus concentration elevates the parathyroid hormone (PTH) release and may cause bone resorption by producing a transient drop in serum ionized calcium (Cashman, 2006). Several studies and investigations tested this for young adults (Calvo et al., 1988; Calvo et al., 1990; Portale et al., 1986). However, due to the high calcium concentration in milk, the ratio of phosphorous to calcium approaches 0.8 to 1.

Calcium phosphate is a very important nutrient in milk. It is poorly soluble in water but can be accommodated in casein to form casein micelles. Thus milk and dairy products are very important sources of calcium, as well as a good source of many other minerals, including trace elements such as zinc.

2.3. Milk protein ingredients: sodium caseinate (SC), and whey protein isolate (WPI)

2.3.1. Sodium caseinate (SC)

Sodium caseinate is a compound derived from casein and exists in an aqueous solution at neutral pH. It is a mixture of casein monomers - α_{s1}-, α_{s2}-, β- and κ-Casein (in a proportion of 4:1:4:1) and small casein aggregates – sub-micelles (Ma & Chatterton, 2021; Ye, 2008). Casein is the main protein in milk, which is found in the form of polydisperse spherical complexes, which also contain colloidal calcium phosphate (CCP) (DeKruif & Holt, 2003). Sodium caseinate is produced from the acidification of casein and subsequent neutralization by sodium hydroxide (Figure 2) (Ma & Chatterton, 2021). The high surface activity of α_{s1}- and β-casein allow sodium caseinate can be rapidly adsorbed on the oil-water interface. As a result, to stabilize the emulsions as an emulsifier (Dickinson, 1994). It is most water-soluble, has a high capacity for water absorption, has melting and foaming properties, etc., thus is widely used in industry for its excellent functional and nutritional properties (Pitkowski et al., 2008).

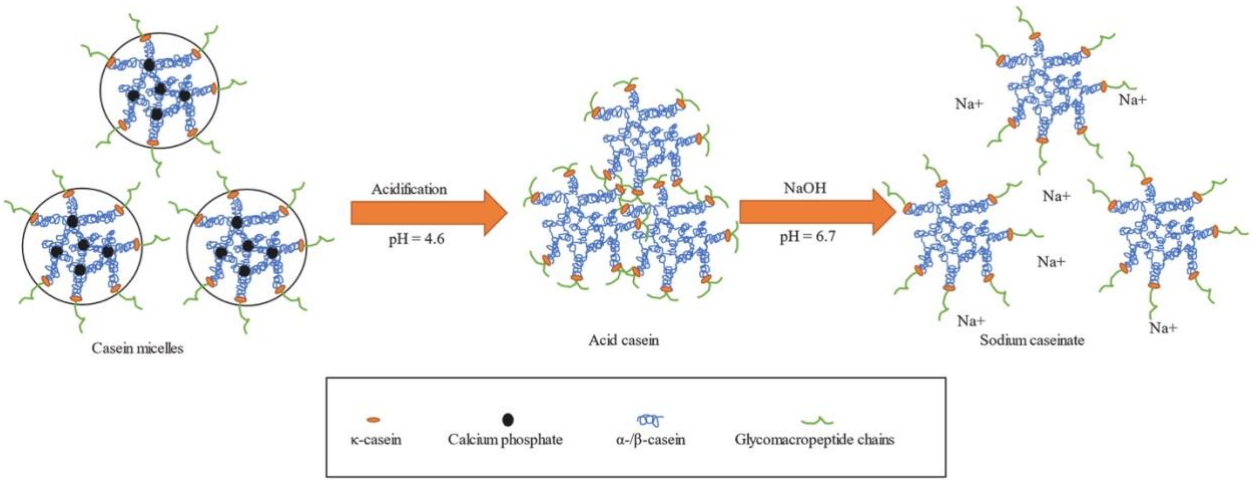

Figure 2. Manufacture of sodium caseinate (Ma & Chatterton, 2021).

Different ratios and sequences of hydrophilic and hydrophobic groups are present in the surface-active caseins. Due to the interaction of steric and electrostatic stabilization, sodium caseinate has been reported to function as an emulsifier or stabilizer; together with the ingestible protein and mild flavor, it is very suitable to be applied in the food industry (Dickinson, 1997; Patel et al., 2010). A study conducted by Patel et al. in 2010 proved that the addition of sodium caseinate enhances the physical stability of the zein colloidal particles dispersion at ambient temperature, which could potentially easily be scaled up in the encapsulating delivering system implemented in food, pharmaceutical, or agricultural formulations (Patel et al., 2010).

It is applied in the food industry as food additives or nutrition supplements; it also can be implemented in as pharmaceutical industry, cosmetic industry, and so on to alter the texture and stability of various products.

2.3.2. Whey protein isolate (WPI)

Whey proteins can generally be commercially categorized in three forms – whey protein concentrate (WPC), whey protein isolate (WPI), and whey protein hydrolysate (WPH), depending on processing techniques (see figure 3.) (Jeewanthi et al., 2015). Whey protein isolate (WPI) has a higher protein content (≥ 90%), and lower fat, lactose, and carbohydrate content compared to whey protein concentrate (WPC), which has a protein content between 29-89%, just like native whey. Whey protein hydrolysate (WPH) is the semi-digested form of the protein (Patel, 2015; Sousa et al., 2012).

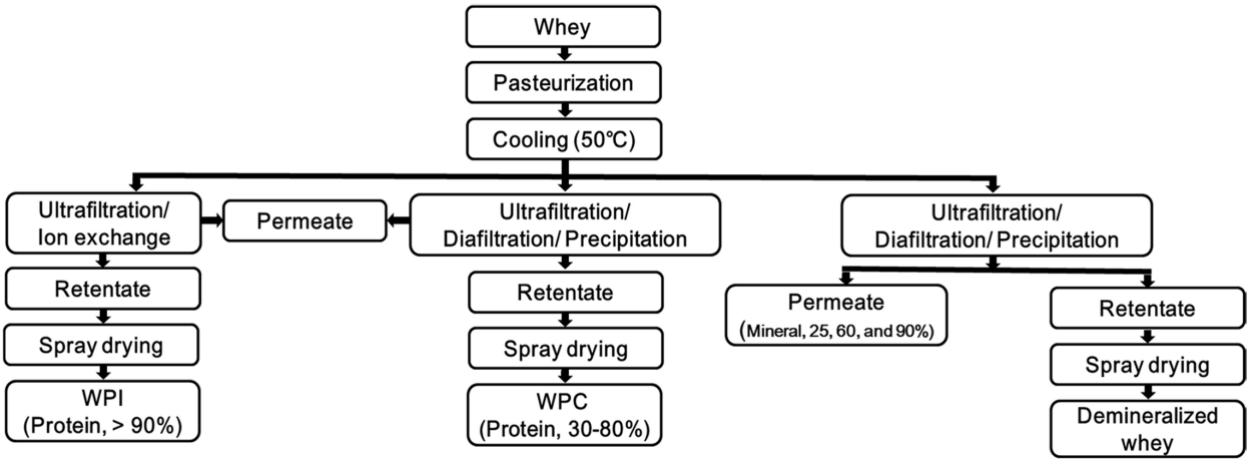

Figure 3. Manufacturing steps of whey products, including WPI (Jeewanthi et al., 2015).

WPI is the primary type that is being employed by a majority of researchers. The low lactose content in WPI is of great importance for lactose intolerance individuals. Furthermore, the low carbohydrate content is also valuable when a low carbohydrate diet is adopted (Hulmi et al., 2010).

To produce WPI, whey needs to be skimmed by microfiltration and demineralized by ionic exchange, electrodialysis or nanofiltration, then further purified by diafiltration. Lastly, concentrate and spray dried the purified retentate (Tsakali et al., 2010). Ion exchange chromatography (IEC) can separate whey protein into two district groups based on their iso-electric points, the negatively charged major whey proteins β-lactoglobulin, bovine serum albumin (BSA), and α-lactalbumin, positively charged minor whey proteins lactoferrin and lactoperoxidase at the pH of rennet whey (pH 6.2-6.4) (Tsakali et al., 2010). Proteins undergo chemical alteration as a result of the ion exchange process, which involves the removal of protein molecules from liquid whey through chemical binding to resins that have been particularly created. Because of the degree of protein denaturation that takes place during manufacturing, ion exchange WPIs tend to have more extraordinary functional attributes like gelling, whipping, and foaming ability (Neville et al., 2001). The relatively mild treatment could also result in higher biological functionality.

WPI has wide applications in food due to its high nutritional, biological, and unique functional properties. For example, a study carried out by Hashim et al. demonstrated that the addition of WPI could not only enhance the structure but also increase the water holding capacity and thus improve the quality of the non-fat yogurts (Hashim et al., 2021). One of the popular products that choose WPI as its protein source is protein bars because of the good-quality protein with little fat or lactose, providing good texture over a long shelf life (Neville et al., 2001).

In some food applications, WPI shows an excellent whip ability and could act as a superior and cost-effective replacement for the egg albumin (Smithers et al., 1996). The potent growth stimulants could also make it a reliable and cost-efficient replacement for costly and quality-unstable fetal bovine serum in the biotechnological and pharmaceutical industries (Smithers et al., 1996). WPI is also frequently chosen as stabilizers in food products like ice creams, frothed drinks, or other food foams and emulsions that are in need of surface-active agents (Onwulata & Huth, 2009).

2.4. Hydroxyapatite (HA) and the interactions with milk proteins

2.4.1. Hydroxyapatite

Hydroxyapatite, the chemical formula [$Ca_{10}(PO_4)_6(OH)_2$], is a hexagonal inorganic crystalline structure composed of calcium and phosphorus and is the main form of calcium present in the human skeleton providing rigidity (Theobald, 2005). Crystalline hydroxyapatite is generally considered to be the final, stable product of calcium and phosphate ions.

Synthetic HA is widely applied in various biomedical applications, especially in the dentistry and orthopedics (Nayak, 2010). Due to the thermodynamical stability of HA and being osteoconductive, together with the similar calcium-to-phosphorus ratio to natural bone and teeth, it has been widely used in hard tissue replacement and some reconstruction utilizations like coatings, bone substitutes, or a drug vehicle of antibiotics and chemotherapeutics to treat bone-associated disease (Bee & Hamid, 2020).

Apart from these applications, the food grade HA only received little attention from the food industry and food scientists due to HA's insoluble characterization and some other factors like the chalkiness affecting the taste. The research from Tercinier, L. in 2012 first disclosed that food grade HA might interact with milk proteins and thereby improve its suspension stability (Tercinier et al., 2013). Arla Food Ingredients developed such a novel product – Capolac containing HA, aiming to utilize this insoluble calcium phosphate salt, expand its implementations and benefit the calcium-fortified applications.

2.4.2. Interactions of milk proteins to hydroxyapatite

Protein adsorption to a solid surface is a common occurrence in many disciplines, and the changes in their structures and functions resulting from adsorption sometimes have a significant consequence. In the presence and absence of other proteins, the adsorption behavior of fibrinogen on the surface of materials such as hydroxyapatite has been widely studied (Nakanishi et al., 2001).

The type of proteins that are adsorbed to the substrate can affect how it behaves. Various molecular weights of proteins have different adsorption behaviors to HA, too (Sharpe et al., 1997). Both nonspecific attractions between protein-positive charges and HA and specific complexing of protein carboxyls with calcium loci on the mineral are involved in the binding (Gorbunoff & Timasheff, 1984). The quality of the HA powder, e.g., particle size, and the specific surface area of the particles have significant influences on the protein adsorption (Rouahi et al., 2006). Thus, several HA particles with various particle sizes were evaluated in this research, see *section 4.2 Different particle size experiment scenarios*.

The interactions between proteins and hydroxyapatite have been widely applied in nano-ceramics, bone replacement, protein separation with high-performance liquid chromatography techniques, and suchlike (Gorbunoff & Timasheff, 1984; Rouahi et al., 2006; Sharpe et al., 1997). However, the interactions between HA particles and milk proteins have not been investigated in detail until a study conducted by Tercinier, L. in 2012 proved that SC and WPI adsorbed on HA particles (Tercinier et al., 2013).

The author of the study examined the adsorption of the main proteins in milk onto the surface of HA particles with a range of tests – zeta potential, confocal microscopy, etc. The main proteins in milk are caseins, and whey proteins, which are sodium caseinate (SC) and whey protein isolate (WPI) powders as the respective protein source. The food-grade HA powder source was tricalcium phosphate (TCP) from Budenheim, Germany (Tercinier et al., 2013).

In this study, the researchers have investigated the surface protein concentration and the surface protein composition of the adsorbed HA pellets. Zeta potential measurements and confocal laser scanning microscopy was also applied to test and observe the adsorption. Then the adsorption process was fitted into two adsorption models, Langmuir and Langmuir-Freundlich, to obtain the best fit model parameters (Tercinier et al., 2013).

Results from the zeta potential and confocal microscopy showed that caseins and whey proteins are bound to HA because of the increased absolute value of the zeta-potential of the particles and the observed images of the particles after mixing the protein and the particles using confocal microscopy. The amount of protein bound to HA particles was calculated by the difference between the protein content in the supernatant and the total amount. A linear relationship between zeta-potential and surface protein coverage for both protein-coated HA was confirmed. Surface protein composition was studied by sodium dodecyl sulfate-polyacrylamide gel electrophoresis (SDS-PAGE). The SDS-PAGE results showed a preference for bindings for individual proteins if the available HA surface is limited. Finally, a suspension behavior was observed with the resuspended HA pellets in water. The number of particles remaining in suspension increased with increased protein concentration (for both SC and WPI) (Tercinier et al., 2013).

All of these experiments conducted for Tercinier's study demonstrated that casein and whey proteins can bind to food-grade HA particles, affecting their colloidal and suspension properties, making the theoretical basis for this study.

2.5. Methods to measure and model the protein adsorption on HA

2.5.1. Methods to measure protein adsorption

The measurement of the adsorption of proteins on solid surfaces can divide into two categories, the amount of adsorbed protein and the conformational changes along with adsorption.

2.5.1.1. Methods to measure the amount of adsorbed proteins

Because the adsorbed amount per unit area is notably low, measuring the amount of adsorbed proteins requires extraordinary precision. Depletion method, one traditional method, the amount of adsorbed protein is determined based on the decrease in protein concentration in the solution after the solid surface has come in contact with the solution. Typically, to be sufficiently accurate, this method requires a large surface area, which is small-particle substances serve as substrates (Nakanishi et al., 2001).

The concentration of the adsorbate in the solution is measured by quantification methods; protein, in this case, is quantified by Dumas methods. Normally the official method to determine nitrogen content in foods is the Kjeldahl method, which consists of a digestion step converting nitrogen (N) into ammonium (NH_4^+), followed by an analytical step where ammonium is quantified by a titrimetry (Simonne et al., 1997). Then a conversion factor is

used to calculate the protein content. However, with drawbacks like time-consuming, and required handling of hazardous waste in this method, a more easy-to-use method -Dumas, has been adopted by a large number of laboratories. This equipment converts all forms of nitrogen into gaseous nitrogen oxides (NOx) by complete combustion in an induction furnace. The NOx gases reduce to N2 which is quantified by thermal conductivity. The protein content is calculated with a conversion factor too. It is time-saving, accurate, repeatable, and could be applied to liquid, semi-solid, or solid samples (Simonne et al., 1997).

Direct measurement of the number of proteins adsorbed on the surface could be done by several techniques, such as radiolabeling, quartz crystal microbalance (QCM), optical techniques like ellipsometry to give average adsorbed protein concentration with refractive index and the thickness of the thin adsorbed film, and so forth (Nakanishi et al., 2001).

2.5.1.2. Methods to measure conformational changes

The structure or conformation of adsorbed proteins has also been investigated thoroughly. Fourier transform infrared reflection (FTIR) could obtain more detailed information on the structure of proteins upon adsorption, FTIR spectroscopy coupled with attenuated total reflectance optics (FTIR-ATR) is also employed to measure the conformational changes, and Atomic microscopy (AFM) can observe the deposits of proteins on graphite and gold surfaces, etc. (Nakanishi et al., 2001).

2.5.1.3. Methods applied in this study

In this study, zeta-potential measurements combined with turbidity measurements using a spectrophotometer or turbidimeter were applied to observe the adsorption of proteins into HA. The surface protein composition and preferential adsorption were defined with sodium dodecyl sulfate polyacrylamide gel electrophoresis (SDS-PAGE).

Zeta potential is the electrostatic potential at the electrical double layer surrounding a nanoparticle in a solution (Clogston & Patri, 2011). It is a common way to evaluate the surface charge and stability of the nanoparticle (Vigneshkumar et al., 2022). The interior of micelles is not uniformly electron dense, and zeta potential is the difference between the external surface of the shell and the liquid. Thus the zeta potential is related to the surface of micelles, which is related to κ-casein, about -20 mV at neutral pH (Crudden et al., 2005; Salopek et al., 1992). For whey protein isolate, the zeta potential was found to be around -20 mV at neutral pH as well (Gbassi et al., 2012). Pure hydroxyapatite is slightly negatively charged, around -11mV; when binding with proteins, this value will aggressively decrease (Tercinier et al., 2013).

SDS-PAGE has a long history of analyzing polypeptide composition in biological materials. The abilities of sodium dodecyl sulfate in binding proteins allow the investigation of polypeptide species, visualized by Coomassie blue staining; this method discovers not only the number of the polypeptide species but also the estimation of the abundance and approximate molecular weight of the species present in a sample (Bischoff et al., 1998).

Two regular protein-reducing agents are used in SDS-PAGE: dithiothreitol (DTT) or beta-mercaptoethanol (BME). The concentration of BME decreases with time because it is volatile and evaporates from the solution. If concentration drops, some protein molecules may not be adequately reduced or become reoxidized, leading to fuzzy bands or spurious artifactual bands.

DTT, on the other hand, is less volatile. Molecule alters from a straight chain to a ring structure during disulfide reduction reaction. Protein sulfhydryls stay reduced once disulfide bonds are broken. Thus lower concentrations of DTT are needed. In this study, DTT was chosen due to the reason listed above.

When choosing the running buffer in SDS-PAGE, the molecular weight of the peptide is considered. Alpha (α)-lactalbumin is the second major protein of bovine whey. It has a molecular weight of 14 kDa and accounts for about 20% of the total whey proteins. Beta (β)-lactoglobulin is a major protein that accounts for approximately 10 to 15% of total milk proteins, it is a globular protein consisting of 162 amino acids (AA) with a relative molecular mass of 18.4 kDa. For caseins, beta (β)-casein has a molecular weight of about 24 kDa, alpha S1(α_{s1})-casein showed a molecular mass of 23.6 kDa, alpha S2 (α_{s2})-casein showed a molecular mass of 25.2-25.4 kDa, beta (β)-casein and kappa (κ)-casein are 24 kDa and 19.2 kDa respectively. Accordingly, buffer 3-(N-morpholino) propane sulfonic acid (MOPS) was picked.

2.5.2. Modeling the protein adsorption on HA

This study aims to investigate whether the protein will adsorb to the HA and Capolac particles. Therefore, adsorption modeling is naturally considered to fit the experimental data. Modeling experimental data is an essential way to predict the adsorption mechanism. Several two-parameter adsorption models, including Langmuir, Freundlich, Temkin, and Dubinin-Radushkevich are commonly applied in adsorption data; only Langmuir and Freundlich will be addressed and involved in this project, because the wide studies on protein adsorption using these two models (Chen, 2015).

The modeled adsorption isotherm typically depicts the adsorption process as a non-linear curve at a constant temperature and pH. The Freundlich model, based on the assumption that energetic surface heterogeneity exists, is the earliest known relationship defining the non-ideal and reversible adsorption that may be implemented in multilayer adsorption. It can be expressed as the equation below, see equation (1) (Chen, 2015; Freundlich, 1906):

$$q_e = K_F C_e^{1/n} \qquad (1)$$

Where q_e is the corresponding adsorption capacity, here indicates the surface protein concentration (mg/m^2), C_e is the concentration of protein solution at equilibrium (g/100g), K_F and n are both the constants to measure the adsorption capacity and intensity respectively. K_F is the Freundlich affinity constant ((100g/g)^N), n is the surface heterogeneity parameter, which means the surface will be energetically homogeneous if this parameter $1/n$ is close to 1 (Tercinier, 2016).

Langmuir model is an empirical model which assumes the adsorption can only take place at a limited number of specific localized spots as monolayer adsorption. It can be stated as equation (2) (Langmuir, 1916):

$$q_e = q_m K_L \frac{C_e}{1 + K_L C_e} \qquad (2)$$

Where q_e is the surface protein concentration (mg/m^2), C_e is the concentration of protein solution at equilibrium (g/100g), q_m and K_L are constants related to adsorption capacity and energy or net enthalpy of adsorption respectively. To be more specific, q_m is the maximum

monolayer surface coverage, K_L is the Langmuir affinity constant (100g/g). This constant denotes a strong protein affinity for the HA and defines the initial slope of the adsorption isotherms (Iafisco et al., 2011).

Langmuir model measures the number of proteins adsorbed onto a surface (HA or Capolac) as a function of the unadsorbed protein concentration once the equilibrium has been established at a specific temperature, making it the most widely used model in the study of protein adsorption on solid surfaces (Mura-Galelli et al., 1991; Tercinier, 2016). This model has to make an assumption that the surface is energetically homogeneous with the same adsorption sites. As described above, it only allows monolayer coverage and no interaction between proteins at the surface.

Freundlich model does not limit adsorption to a monolayer and can be applied in multi-layer adsorptions. Some studies have shown that the Freundlich model fits better for the Bovine serum albumin (BSA) adsorption on HA at high initial protein concentration based on the assumption that the protein adsorbing in multiple layers often causes surface energy heterogeneity (Mavropoulos et al., 2011).

The outcomes of the modeling are anticipated to offer a particular theoretical foundation for the operational design and practical application of the adsorption systems for Capolac and therefore improve its suspension stability.

3. Material and methods

The aim of the study is to investigate the adsorption ability of milk protein casein and whey to hydroxyapatite particles and a similar product, Capolac from Arla Foods Ingredients. The source of casein is sodium caseinate (SC, C-8654-500G), which was acquired from Sigma-Aldrich Chemie GmbH, Germany. Whey protein isolate (WPI, 90% protein, Lacprodan® DI-9213) was obtained from Arla Foods Ingredients, Viby J, Denmark. Hydroxyapatite powders have three batches with different particle sizes; batch1 (HA1) and batch 2 (HA2) (391947-100GM) were obtained from EMD Millipore Corp, an Affiliate of Merck KGaA, Darmstadt, Germany. Batch 3 (HA3) (MKCQ4259, 900204-50G) was purchased from Sigma-Aldrich Chemie GmbH, Germany.

The product Capolac was received from Arla Foods Ingredients Group P/S, Viby J, Denmark.

Methods to investigate the adsorption were inspired by the study of Terciner 2012 (Tercinier et al., 2013) and based on the available laboratory facilities in the food department of Copenhagen University. First, the HA powders need to be verified on the adsorption of protein, and then tested and compare with the product Capolac from Arla Food Ingredients. In order to compare the powders, particles need to be analyzed; in this case, the particle size was investigated. And in order to examine whether the protein will adsorb on the different particles, two different protein/powder suspensions were prepared for further investigation. Both supernatants and the HA pellets were useful when testing in different lab scenarios.

Methods chosen to test the adsorption include zeta-potential measurements, SDS-page, turbidity measurements, and finally, the suspensions are visually observed to verify whether the suspension stability has improved by adding protein solutions. More clarifications could be found in the theoretical background *section 2.5.1 Methods to measure protein adsorption.*

Detailed explanation and describing of different steps and experimental settings are elucidated below.

3.1. HA particle characterization

HA particle had divided into three batches with different particle sizes. The particle size of each batch was measured with a Malvern Mastersizer 3000 (Malvern Instruments Ltd., Malvern, Worcestershire, UK). The powder of batch 1 (HA1) was from EMD Millipore Corp; batch 2 (HA2) was ground particles from batch 1 powder. Batch 3 (HA3) was from Sigma-Aldrich Chemie GmbH, Germany.

The procedure to use Malvern Mastersizer 3000 is summarized as follows: first, a suspension of HA powder in water (1% w/w) was prepared, then introduced drop by drop into the wet dispersion unit of the Mastersizer until the desired obscuration (between 10- 20%) was reached. A refractive index of 1.63 and an absorption factor 0.001 were applied to calculate the particle size distribution. These parameters were chosen based on a previous study from Terciner. Finally, the median particle size d_{50} was recorded for all batches. An average of six measurements was employed for all the samples.

Batch 1 (HA1) and batch 2 (HA2) adopted a reported specific surface area of the powder, 65 m^2/g. Although the ground particle may end up in a different specific surface area, the particle size differ not sharply, therefore the same specific surface area was adopted. The specific surface area of batch 3 (HA3) and Capolac (CA) was obtained from the supplier, which is ≥ 80 m^2/g.

3.2. Protein/HA suspension preparation

To prepare for the subsequent measurements, two methods were used to prepare the suspensions; one is a constant amount of HA powder added to different concentrations of protein solutions (both SC and WPI), to be used in the measurement of zeta potential, turbidity and suspension behavior observations. The other one is a constant amount of protein added to different concentrations of HA suspensions, to be used in the SDS-PAGE experiment.

Method 1: a constant amount of HA (~1g) was added to 9g of different concentrations of protein solutions (from 0.5 – 4%). A control was prepared by adding 1g HA to the same amount of Milli-Q water. Protein solutions were prepared with different amounts of proteins added to Milli-Q water. The stirred (at least 1 hour) solutions were left overnight in the fridge (at 4°C) for complete hydration. Raw data on different protein solutions see *Appendix 2*.

Method 2: a constant amount of protein (100μL 1% w/w SC or WPI) was added to 900μL different concentrations of HA suspensions (0.1- 3% w/w). A control was made by mixing 100μL protein with 900μL Milli-Q water.

Both suspensions were stirred for 2 hours at room temperature, then centrifuged at 3000 rpm for 20 minutes. Then supernatants were poured out, weighed, and saved for later analysis. The HA pellets were weighed and saved for later analysis as well.

The same procedure applies to all the HA or Capolac/protein suspensions.

3.3. Determination of surface protein concentration

The supernatants of constant HA/Capolac with different concentrations of protein suspensions were analyzed for total nitrogen content using the Dumas method. Each supernatant sample from all the suspensions was weighed roughly the same amount and transferred to the combustion cell of the Dumas analyzer. The recorded sample weight (~0.5g each) was registered in the computer while the measurement proceeded, then the nitrogen content was obtained by the Dumas analyzer and the data was saved for further calculation. This nitrogen content value for HA and Capolac could be found in table A2 & A3, respectively in *Appendix 2*.

The protein content was calculated by a conversion factor of 6.38 to convert the nitrogen content acquired by Dumas. This conversion factor was adopted and was the same as the previous study done by Tercinier et al. (2012).

After all the weighing and calculation, the surface protein concentration (mg protein/m^2 HA) was calculated with the formula below:

$$\text{Surface protein concentration} = \frac{m_i[p_i] - m_{sup}.[p_{sup}] - (m_{wetsed} - m_{drysed}).[p_{sup}]}{m_{drysed}.[SA_{HA}]} \times 10 \quad (3)$$

Where m_i is the mass of the initial protein solution (g), m_{sup} is the mass of the supernatant (g), m_{wetsed} is the mass of wet HA pellets acquired after centrifugation (g), m_{drysed} is the mass of dry HA powder which added to the initial protein solution (g), p_i is the concentration of initial protein solution (g/100g), p_{sup} is the measured protein concentration of the supernatant (g/100g), SA_{HA} is the surface area per gram of the HA/Capolac powder (65 m^2/g/ 80 m^2/g). The raw data and parameters for the calculation see *Appendix 2*.

3.4. SDS-PAGE to determine the remaining protein in the supernatants

To further analyze the adsorption of different proteins bound to the HA powder, the supernatants of constant protein with different concentrations of HA/Carpolac suspensions were performed with sodium dodecyl sulfate polyacrylamide gel electrophoresis (SDS-PAGE).

To prepare for the SDS-PAGE sample, the protein content of the supernatants was first measured with Nanodrop. Nanodrop is a spectrophotometer that can quantify the protein sample with only 1-2 μL in only 3 seconds. This is just a rough estimation to facilitate the following procedure, to calculate the proportion of the LDS buffer according to the protein concentration.

Once the protein content was determined, the SDS-PAGE samples were prepared by mixing the LDS sample buffer, reducing agent DTT, and the supernatant samples to a final concentration of around 1mg/mL sample according to the protein content of each suspension.

Then the samples were heat treated with a thermal mixer for 5 minutes at 95°C. After that 6 μL of samples were loaded in a 15-well gel, and the gel was running at 200V for around 40 minutes with an electrophoresis unit.

When the gels finished running, the power was disconnected, and the gels were stained with Coomassie and stayed overnight on a rocking table in a fume hood. After staining, the gels were scanned with a gel scanner when the bands appeared nice and clear.

3.5. Zeta-potential measurements

The HA pellets obtained after centrifugation were resuspended in Milli-Q water at a concentration of 0.5% w/w for zeta-potential analysis. A Malvern Zetasizer Nano-ZSP instrument and a reusable zeta-potential cell (Malvern Instruments Ltd., Malvern, Worcestershire, UK) were used to determine the zeta potential of the resuspended particles.

The measuring cell was placed in the instrument after receiving the transferred sample. The temperature of the cell was kept at room temperature (around 20°C). The parameter of the devices was set with a voltage of 80V, and the calculation was based on the Smoluchowski model. Each measurement has four duplicates.

3.6. Turbidity measurements

The turbidity measurements were conducted with two different instruments to verify the consistency of the results from different methods and reduce human error, which is very likely to happen during the measuring process. One is the spectrophotometer Evolution 300 UV-Vis from Thermo Electron Corporation (Thermo Electron Scientific Instruments LLC, Madison, WI, USA). The other one is a Hach 2100N turbidimeter (Hach Lange AB, Solna, Sweden).

The HA pellets were resuspended in Milli-Q water at a concentration of 0.125%, transferred to a 1mm disposable plastic cuvette, and then placed in the spectrophotometer. Absorbance value at a wavelength of 900 nm, which can indicate the change in the turbidity of the samples, was recorded over 200 minutes. Then the reduction in absorbance was calculated with the formula listed below:

$$\text{Reduction in absorbance} = \frac{A_t}{A_0} \times 100 \qquad (4)$$

Where A_t is the absorbance at time t, A_0 is the initial absorbance.

When using the turbidimeter, the resuspended samples were transferred to the glass cells of the turbidimeter, then the glass cells were placed in the instruments, and values with a unit NTU (Nephelometric Turbidity Unit) were recorded over 200 minutes. NTU signifies that the turbidimeter measures the sample's scattered light at a 90-degree angle from the incident light. Then the reduction in the scattered light was calculated using the same formula (4) applied to the spectrophotometer.

In the meantime, the HA/Capolac pellets were resuspended in Milli-Q water at a concentration of 10% w/w, left undisturbed at room temperature for 24 hours, and the suspension of different concentrations of HA pellets was photographed in order to observe the suspension behavior of different pellets.

3.7. Statistical analysis

Data analysis, including the relationship between surface protein coverage and zeta potential, regression analysis, ANOVA, and Tukey test, were analyzed by Excel (Version 16.63.1).

The experimental data were fitted with the adsorption model, Langmuir model, and Freundlich model using software R (version 4.2.1).

To evaluate the data and determine which model fits better, two parameters – the correlation coefficient (r^2) and standard errors (S.E.) need to be reviewed and compared. The correlation coefficient (r^2) is usually used to determine the best-fitting isotherm to the experimental data, exhibited in the equation below:

$$r^2 = \frac{\sum(q_m - \overline{q_e})^2}{\sum(q_m - \overline{q_e})^2 + \sum(q_m - q_e)^2} \quad (5)$$

Where q_m is the constant obtained from the isotherm model, q_e is the equilibrium capacity obtained from lab data, $\overline{q_e}$ is the average of q_e.

4. Results and discussion

4.1. HA particle characterization

In order to evaluate the difference between the three batches of HA and Capolac, the particle sizes were measured. The results of the three batches of HA particles are listed as follows: batch 1 (HA1) – the median particle size d_{50} was found to be 64.2 μm, batch 2 (HA2) – the median particle size d_{50} was found to be 36.4 μm, batch 3 (HA3) - the median particle size d_{50} was found to be 4.99 μm (see figure 4A-C).

Capolac (CA) showed a median particle size d_{50} of 3.92 μm, the most similar to HA particle batch 3 (see figure 4D).

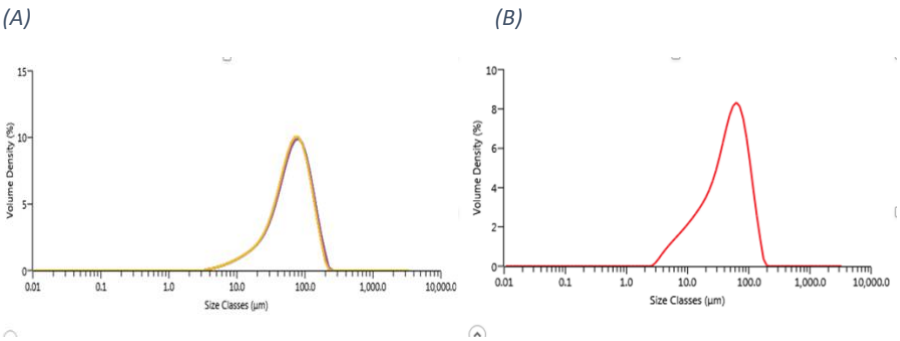

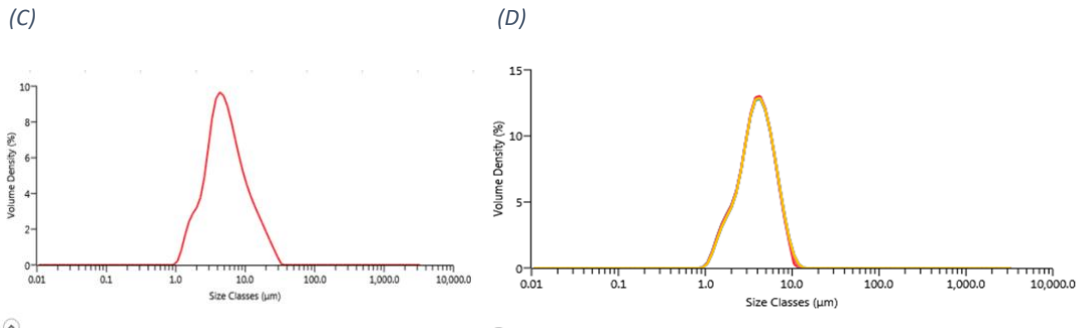

Figure 4. Graphic display of the median particle size d_{50} of the different HA particles and Carpolac: (A) HA, batch1 (HA1); (B) HA, batch 2 (HA2); (C) HA, batch 3 (HA3); (D) Capolac (CA).

The particle size of the four particles, and specific surface area are summarized in table 5 below.

Table 5. Summary of the particle size and specific surface area for the four particles.

Batch	Particle size (d_{50}) (µm)	Standard deviation	Specific surface area (m^2/g)
HA1	64.2	1.3511	65
HA2	36.4	0.1553	65
HA3	4.99	0.0063	80
CA	3.92	0.0281	80

From the particle size graph, it can be found that the first batch of HA has the biggest particle size, which is massively more than batch 3 and Capolac, even double batch 2. This could indicate a different experimental outcome, as the surface area of the powder could differ significantly, consequently affecting the suspension ability of the particles, which will be further investigated in a later section. Batch 2 has a smaller particle size; however still considerably larger than batch 3 and Capolac. The particle size of Capolac is most similar to batch 3, which signifies that the outcome of these two powders would be the most closely, which will be testified in different experimental scenarios.

4.2. Different particle sizes experimental scenarios

To evaluate if there is a difference in protein adsorption onto the different sized HA, the three batches of HA powder were tested zeta-potential, performed SDS-PAGE, and observed the suspension behavior respectively. It turns out the last batch (HA3) powder, which has the smallest particle size, the experimental outcome was the most similar to the reference article (Tercinier et al., 2013). Some of the results were selected and presented below, just for comparison of the different particle sizes affecting lab results.

4.2.1. Zeta potential

A comparison of zeta-potential measurements of the three batches is shown below; see figure 5. The original data for the different tests are presented as graphs which can be seen in *Appendix 3*. Only batch 3, which is the closest particle size to Capolac, will be displayed in the later section as a control group to compare with Capolac.

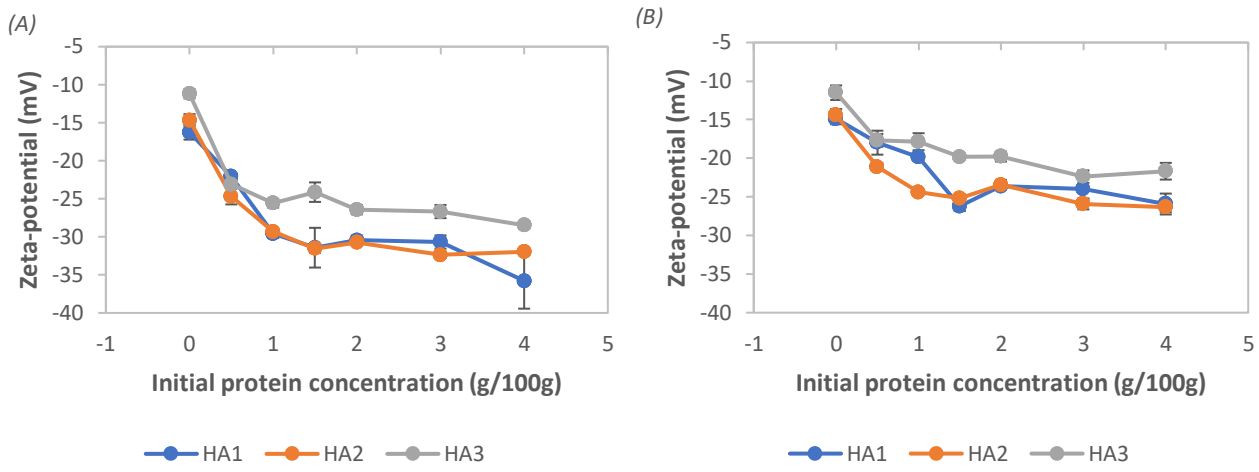

Figure 5. Zeta potential of the three different batches of HA powders for both SC and WPI: (A) SC with different batches of HA; (B) WPI with different batches of HA.

It can be seen from the graphs that all three particles have a similar rough trend for SC and WPI, respectively, which are the maximum absolute zeta potential for SC and are all larger than the value for WPI, and they all increased with increased protein concentration. The first batch (batch 1) with the biggest particle size shows an original value of about -17mV, and the absolute value increased gradually with the increased protein concentration until it reached a maximum value of -38 mV for SC and -28 mV for WPI. The second batch (batch 2 – ground HA) shows an original value of -15 mV and reached a maximum value of -32mV for SC and -28mV for WPI. This one exhibited a more distinct raise when added protein and a more apparent trend until it reached the maximum value compared to the first batch.

The last batch started with around -11mV for pure HA particles, and the absolute value increased sharply with added protein until it reached a maximum value of -28mV for SC and -22mV for WPI. These values correspond with the theoretical value of pure HA with a zeta-potential around -11mV, and when added protein, the value will reach for SC and WPI.

A two-way ANOVA test was conducted for SC and WPI, respectively, to see if there was a significant difference between the different particles. The original summary table can be seen in *Appendix 4*. From the analysis results, both SC and WPI showed substantial differences between the different particles, meaning the different particle sizes play an important role in the adsorption ability of proteins.

A turkey test was performed to further investigate the comparison of the particle size within different groups. The results of the analysis can be seen in table A6, A7 in *Appendix 4*. According to the analysis result, a significant difference could found between HA1 and HA3, HA2 and HA3 for both proteins, but no significant difference between HA1 and HA2. This could be due to batch 2 was the ground particles from batch 1, they were actually the same particle from one supplier. The particle size of HA2 was only half of the HA1, but HA3 was a new particle that only has one tenth of the first particle size, indicating the discrepancies should be large enough to observe the difference. That is why the third batch HA3 was the best among all the three batches in suspension stability.

The results for the three batches have demonstrated that the smaller the particles, the better outcome, which is the better suspension stability. From batch 1 to batch 3, the particle size reduced; accordingly, the zeta-potential changes. The smallest batch presented the most accurate and evident tendency value of zeta-potential, which further proved that both SC and WPI could obviously adsorb to the pure particles.

4.2.2. SDS-PAGE

The results for SDS-PAGE of the three batches can be seen in figure 6.

(A)

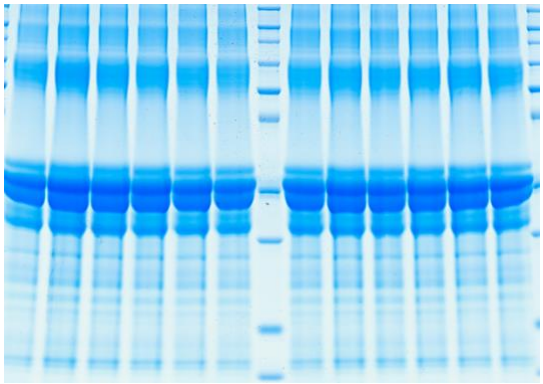

(B)

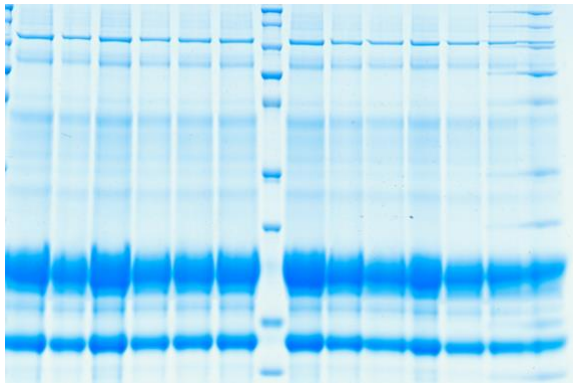

(C)

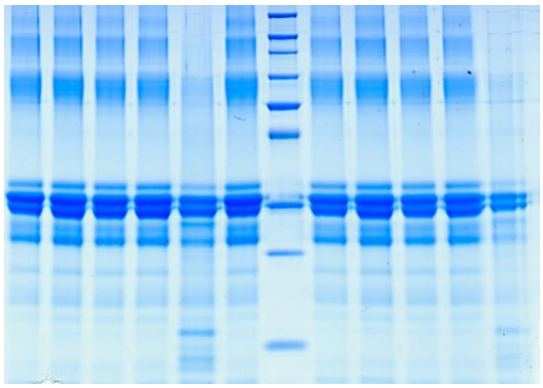

(D)

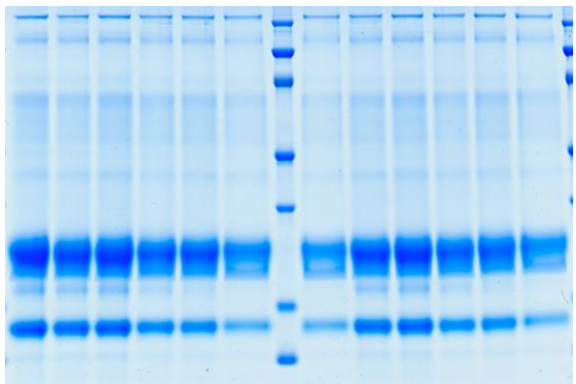

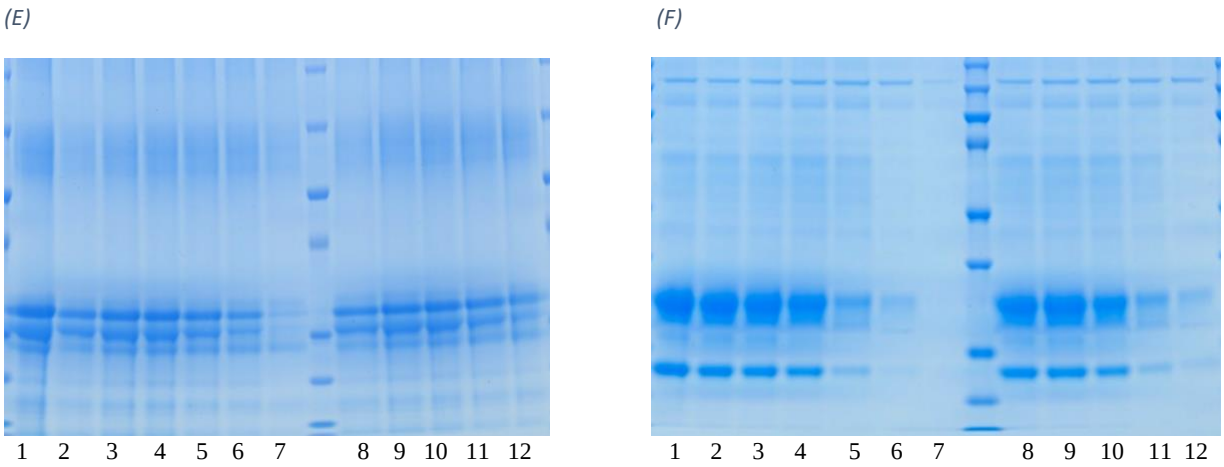

Figure 6. Gel images of the supernatant for the three batches of HA powders/protein suspensions for SC and WPI: (A) HA1, SC; (B) HA1, WPI; (C) HA2, SC; (D) HA2, WPI; (E) HA 3, SC; (F) HA3, WPI.

In those images, the HA concentrations are increasing from left to right (lane 1 to lane 7). Lane 1 is the control group without adding HA; lane 2 to lane 7 are from concentration 0.1% w/w to 3% w/w of HA. From lane 8 to lane 12 is just a repeatable concentration from 0.1% w/w to 2% w/w. If the color of the bands is lighter, which means less protein remains in the supernatants; in other words, more proteins are adsorbed on the HA particles.

In the first batch, which has the largest particle size, both gel images for SC and WPI (figure 6A, 6B) look like overloaded. Therefore, it is difficult to see the discrepancies between the different concentrations, only a slightly lighter color for higher concentrations could be found in the gel image for WPI suspensions.

In the second batch, with medium particle size, a precise observation can be found in higher concentrations of HA; the color is lighter than in lower concentrations, which implies the protein is evidently adsorbed to the particles in higher HA concentrations of suspensions for both SC and WPI.

The last batch is also the smallest particle size; a distinct color gradient could be observed for both SC and WPI suspensions; the higher the concentration of HA, the more disappearing the colors, particularly for the highest concentration (lane 7 in figure 6E, 6F), the band is almost invisible, indicating the barely protein remained in the supernatant after the mixing and centrifuge of the two powders.

A remarkable difference was discovered for the three batches of HA powders from the gel images exhibited above; this is following the zeta-potential measurements results, indicating the smaller particle size, the more easily it will adsorb to the proteins.

4.2.3. The suspension behavior observations

Figure 7 demonstrates the suspension photo of the three different particles resuspended in Milli-Q water after 24 hours undisturbed.

(A)

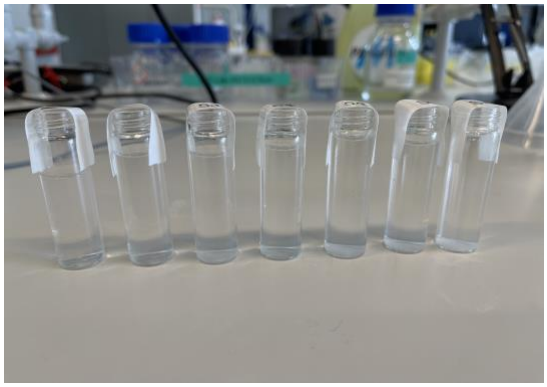

(B)

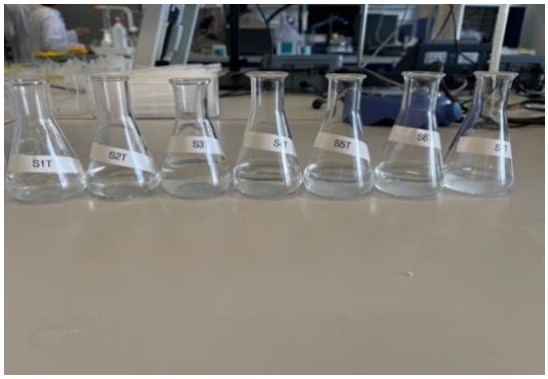

(C)

(D)

(E)

(F)

Figure 7. Suspension photos of the three batches of HA powders: (A) HA1suspended in SC; (B) HA1 suspended in WPI; (C) HA2 suspended in SC; (D) HA2 suspended in WPI; (E) HA3 suspended in SC; (F) HA3 suspended in WPI. From left to right, the protein concentration increases. The first sample on the left is always the control group with water.

Corresponding to the results of SDS-PAGE, the contrast for the suspension photos was very similar to the gel images of the three particles. For the first batch with the biggest particle size, it is very hard to notice the discrepancies in the suspension behavior with increasing protein concentration. Only a slight turbidity was observed in suspensions with higher protein concentration, especially for WPI (figure 7B).

In the next batch with medium particle size, it is easy to see the turbid suspensions with added proteins compared to the control. However, a distinct gradient and the degree of the turbidity were not manifest for different protein concentrations.

Batch 3, the smallest particle size batch, demonstrated an obvious and evident turbidity gradient, with increased protein concentration (both SC and WPI), the opaquer of the suspensions. This trial further proved that the protein could adsorb on the particles, and with increased protein concentration, the better suspension stability it could contribute.

As Barone et al. recently reported in a review, some physical modifications, for example, reducing the particle size of such insoluble calcium salts like hydroxyapatite, would increase the suspension stability of whey protein-based products during the processing and storage (Barone et al., 2022). This experiment scenario also demonstrated that not only did whey protein increase the suspension stability, but sodium caseinate also behaved better in the suspension stability under the addition of hydroxyapatite.

From the suspension pictures, a sediment layer could be discovered. This sedimentation of the insoluble calcium salts, here the HA particles, would likely happen during the storage, especially when the product's shelf-life is long. This phenomenon could be explained by Stoke's law under ideal conditions; see *equation 6* (Barone et al., 2022).

$$\mu = \frac{d^2 g\,(\rho_s - \rho_f)}{18\eta} \qquad (6)$$

Where μ is the sedimentation rate of the suspended particles, d is the particle size diameter, ρ_s is the particle density, ρ_f is the density of the dispersant phase, and η is the product viscosity. As stated in this equation, the sedimentation rate could be reduced by either increasing the product viscosity η by adding hydrocolloids or reducing the particle diameter d. By decreasing the particle size, the sedimentation of the particles slowed down, which improved their suspension capacity.

4.3. Determination of surface protein concentration

Surface protein concentration was calculated by the formula listed in *section 3.3 Determination of surface protein concentration.* The results of *section 4.2* have suggested that only batch 3 of HA particles are close to the research findings of Tercinier, L. in 2012 because of the similar particle size of the powders, thus only batch 3 will be present in this unit, and henceforward to compare with the product Capolac from Arla Food Ingredients.

The amount of protein bonded to the HA or Capolac particles differs due to different protein concentrations. This amount was calculated by the difference between the total protein and supernatant protein content (formula 3). Both adsorption of SC and WPI to the powders are present in the same graph (figures 8 & 9) as a function of the initial protein concentration.

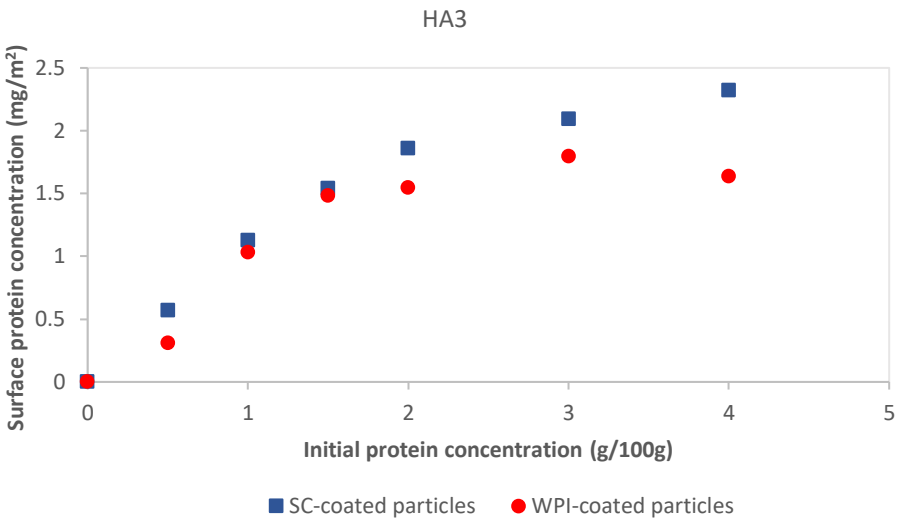

Figure 8. Surface protein concentration (mg/m^2) of HA particles as a function of protein concentration.

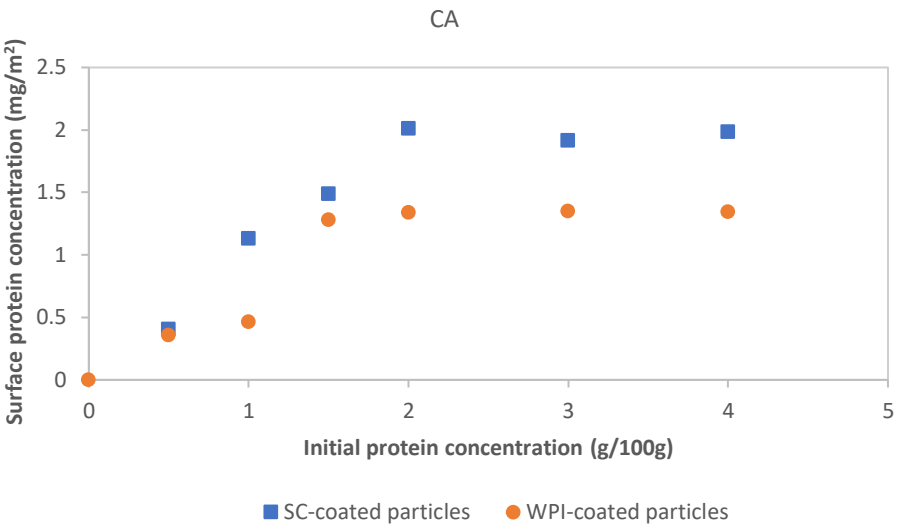

Figure 9. Surface protein concentration (mg/m^2) of Capolac particles as a function of protein concentration.

Figures 8 and 9 show that all the particles mixed with proteins (SC and WPI) increased gradually with increased protein concentration until they reached a maximum coverage value. HA particles mixed with SC reached a maximum value of around 2.5 mg/m^2 when the initial protein concentration arrived at 2% (w/w) and remained unchanged. The other one, mixed with WPI, achieved a lower coverage maximum value of about 1.8 mg/m^2 at a concentration up to 1.5% (w/w). This is also a similar value and trend to Lucile Tercinier et al. (2013)'s findings and a further verification of their results.

Capolac demonstrated a similar pattern to HA for both SC and WPI-coated particles. For particles blended with SC, it arrived at a maximum coverage value of approximately 2.5 mg/m^2 at a threshold protein concentration of up to 2% (w/w). For WPI-coated particles, the surface coverage maximum value was around 1.6 mg/m^2 at the highest protein concentration of 1.5% (w/w).

The higher surface protein coverage for SC than WPI could be due to the higher molecular weight (MW) of casein than whey protein, in other words, the greater interaction area. Capolac has a similar particle size to HA, meaning a similar surface area. Therefore, the surface protein coverage is similar in both particles for SC and WPI, respectively.

4.4. SDS-PAGE to determine the remaining protein in the supernatants

The supernatants of various concentrations of HA or Capolac added to a constant amount of protein (SC/WPI) were analyzed by SDS-PAGE. The scanned gel images are shown below (figures 10 &11.).

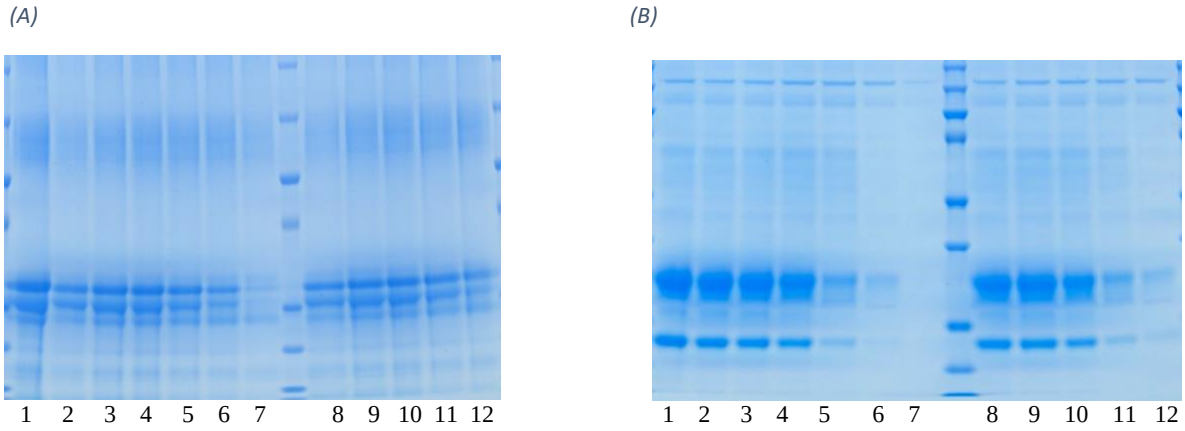

Figure 10. Gel images of the supernatant of HA powders suspended in SC/WPI protein solutions: (A) HA3 in SC; (B) HA3 in WPI.

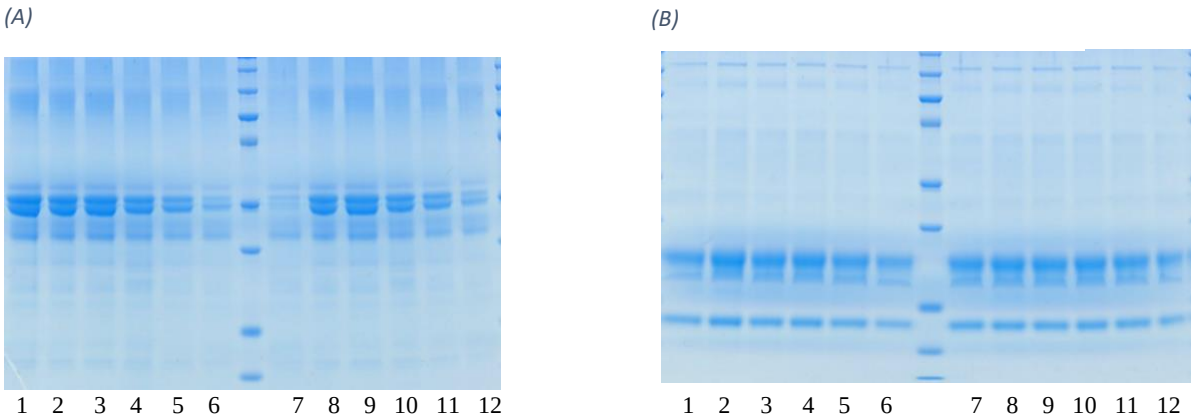

Figure 11. Gel images of the supernatant of Capolac powders suspended in SC/WPI protein solutions: (A) CA in SC; (B) CA in WPI.

As described in *section 4.2.2 SDS-PAGE*, a noticeable color gradient for the bands could be found for the HA3 powders for both SC and WPI, indicating the potential adsorption of the HA powder to the proteins. Compared to this, the gel images of Capolac suspended in SC displayed an even more distinct color diminishing with the increased HA concentration, denoting the adsorption ability of this powder to Sodium Caseinate. For Whey proteins, the bands in the gel images were not evident as compared to SC or the WPI for HA powders. Still, the higher HA concentration got a lighter-colored protein band. This implies that potential protein adsorption for WPI would happen with large possibilities in higher HA concentrations.

Both results proved that increased HA concentration decreased the remaining protein in the Capolac suspended in SC/WPI supernatant. In other words, the particles were adsorbed onto the proteins in the HA pellets that will be resuspended in water for further observation. If the assumption that the Capolac would evidentially adsorb to the Sodium Caseinate than WPI, a remarkable turbidity difference would be expected for the SC resuspension photos than those of WPI photos.

4.5. Zeta-potential measurements

The obtained HA or Capolac pellets, after centrifugation of the mixed constant HA with different protein suspensions, were resuspended in water at a concentration of 0.5% (w/w) and measured the zeta potential with a Malvern Zetasizer. Acquired results for HA3 and Capolac were illustrated below (see figures 12 &13.). The original graphs for all four samples are exhibited in *Appendix 5*.

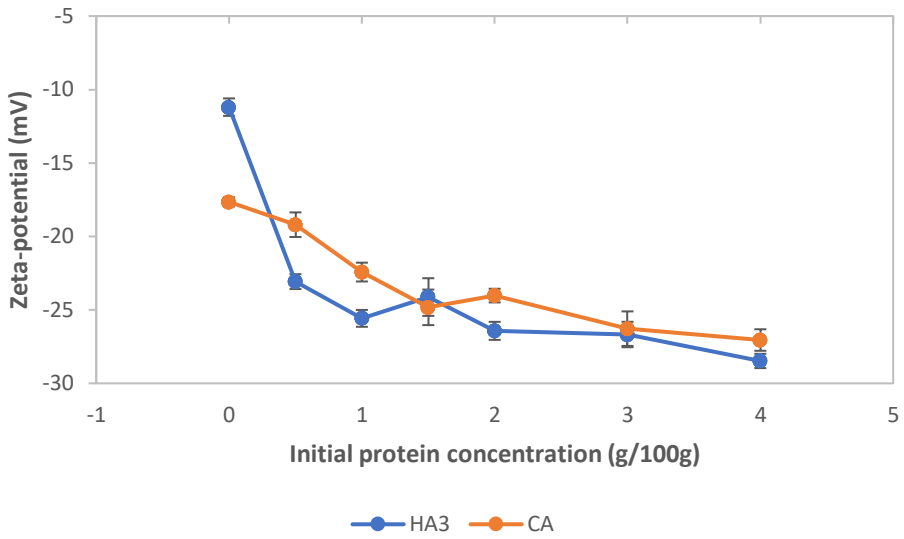

Figure 12. Effect of different protein concentrations on zeta-potential of HA or Capolac particles suspended in SC.

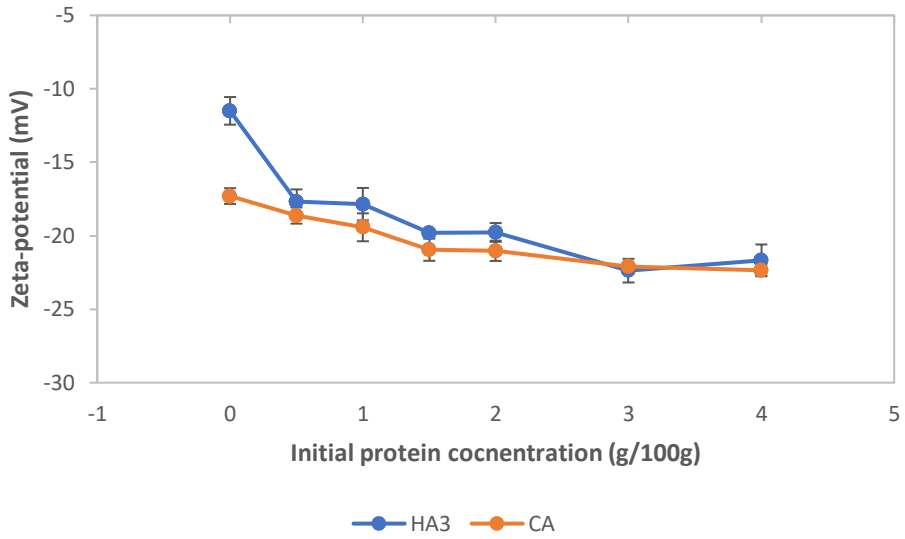

Figure 13. Effect of different protein concentrations on zeta-potential of HA or Capolac particles suspended in WPI.

Figure 12 and 13 demonstrated that absolute zeta-potential for both HA and Capolac was increased (more negative value) with increased initial protein concentration. Pure HA was negatively charged when suspended in water, at a value of roughly -11 mV in both graphs for SC and WPI (figure 12 &13.). The absolute value increased (more negatively) when the protein was added to the particles until it reached the maximum value of -28 mV for SC at a concentration of 2% (w/w) and -22 mV for WPI at a protein concentration of 1.5% (w/w). At higher protein concentrations, the zeta-potential value was maintained more or less the same when the maximum value was achieved.

For Capolac powder, the original Capolac particle suspended in water presented a zeta-potential of around -17 mV for both SC and WPI mixed suspensions, larger than pure HA particle in the absolute value. Then the value increased with the addition of protein until it reached the peak value of -28 mV at a concentration of 3% (w/w). For WPI blended suspensions, the zeta-potential value expanded to nearly -22 mV at a protein concentration of 1.5% (w/w).

Results from the graphs indicate a similar trend for SC or WPI suspensions for both HA and Capolac particles, except for the original value of pure particles. Both SC-coated particles reached a threshold value of -28 mV; for WPI-coated particles, both HA and Capolac arrived at a top value of -22 mV, which is lower than SC. The critical protein concentration of the zeta-potential plateau value reached for WPI is almost the same, with no more increase after a concentration of 1.5% (w/w). For SC, there was a slight difference, at a limit concentration of 2% (w/w) for HA and a concentration of 3% (w/w) for Capolac.

A two-way Anova test was conducted to compare the data for the HA3 and CA particles suspended in both SC and WPI. The average data and the summary table for the Anova test can be found in *Appendix 6*. According to the analysis, both particles suspended in SC or WPI showed no significant differences, which means the Capolac demonstrated a similar adsorption pattern to HA.

The decrease in zeta-potential value indicates that both caseins and whey proteins had adsorbed to the surface of the HA and Capolac powders since both proteins are negatively charged at neutral pH.

According to a study by Branko Salopek (1992), the greater the absolute value of zeta-potential, the more stable the particle is. This research revealed that the size of the zeta potential could be an indicator of change in the suspension stability. Because the suspension stability is related to the changing interaction of attracting forces on one side and repelling forces on the other depending on the particle distance. The surface potential value could be obtained by adding the attracting or repelling energies. High zeta potential gives raise to the electrostatic repulsions between the particles, this correlates with the small sedimentation volumes, in other words, a stable system (Gallardo et al., 2005). The maximum precipitation was found at the value around zero, and with increased zeta-potential absolute value, the stability was improved, around -80 to -100mV the stability was discovered to be extremely good. If one would destabilize the particle suspension, one possible way is to lower the zeta potential, like reducing the electronegativity of a particle (Salopek et al., 1992). This means Capolac is more stable than HA, and SC-coated particles are more durable than WPI-coated particles.

Pure HA was just hydroxyapatite, but Capolac is a product with around 70% of hydroxyapatite, and the rest contains a certain amount of minerals such as sodium, magnesium, potassium, and chloride. Besides these cations and anions, the product also includes macronutrients like lactose, fat, etc. All these elements make Capolac more stable because the particles may already be partly coated; in other words, they increase the absolute value of zeta-potential.

The higher zeta-potential absolute values for SC than the WPI indicate better adsorption of SC onto the HA/Capolac particles than WPI. This could be due to the higher MW of casein than the MW of whey protein, in other words, the greater interaction area. Also, the phosphoryl groups on casein will strongly interact with the positively charged part of the HA/Capolac surface particles (Barone et al., 2022; Juriaanse et al., 1981).

4.6. Turbidity measurements and suspension behavior

The resuspended HA pellets or Capolac pellets (concentration 0.125% w/w) were analyzed by both spectrophotometer and turbidimeter to test the suspension ability of the particles through the reduction in absorbance and the reduction in scattered light over 200 minutes.

After the measurement of the absorbance of each sample, the reduction in absorbance was calculated with the formula (2) listed in *section 3.6,* displayed in figures 14-17.

(A)

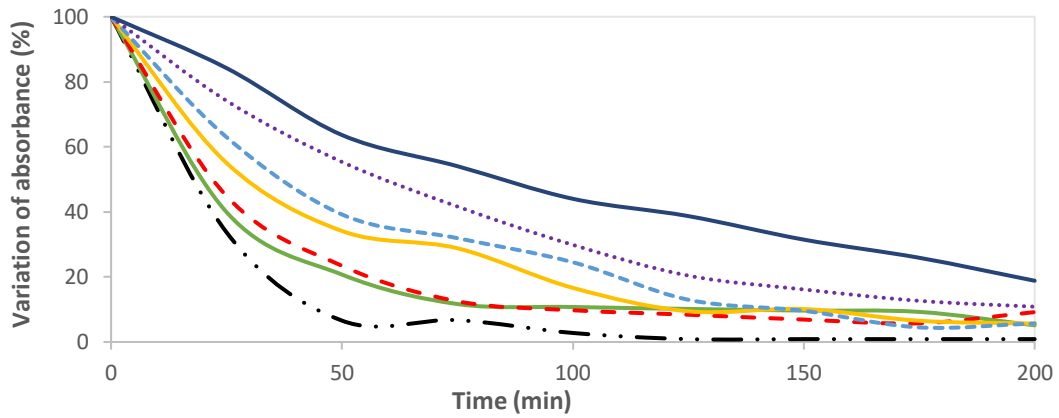

(B)

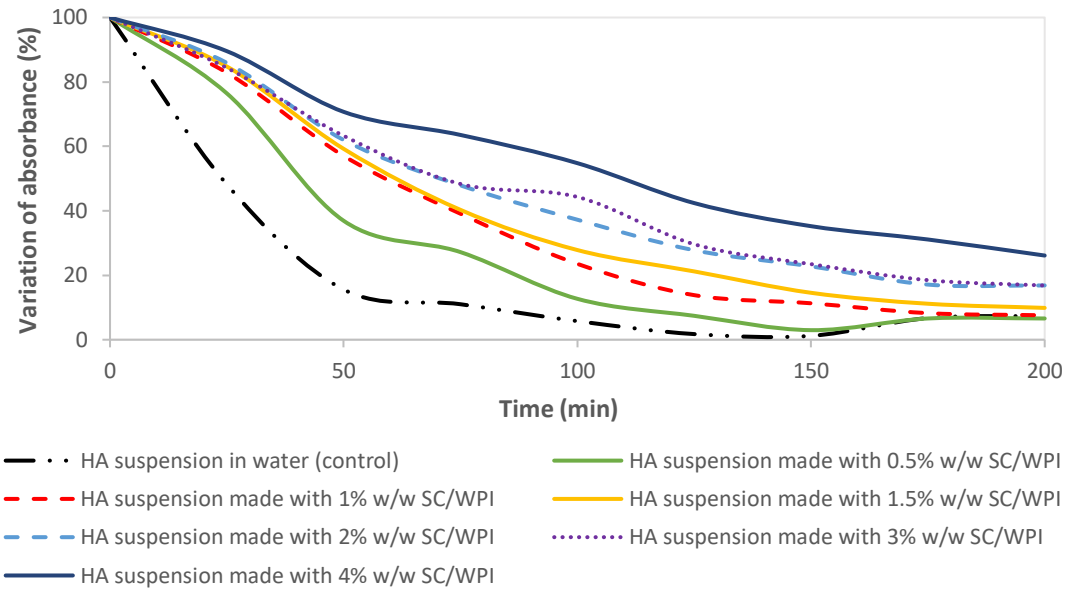

Figure 14. Absorbance as a function of time of suspension of HA3 particles (0.125% w/w) made with different concentrations of SC/WPI solutions: (A) SC; (B) WPI.

Figure 15 shows photographs of the resuspended HA/Capolac pellets in Milli-Q water after 24 hours with no disturbance.

(A) (B)

Figure 15. Suspension photos of the HA3 pellets in water: (A) HA3 with SC; (B) HA3 with WPI. From left to right, the protein concentration increased. The first one on the left is the control group without adding protein.

Figure 14 shows that within 200 minutes, the absorbance of the control group of HA (black dashed line) reduced to less than 5% of its original value. The suspension photo also proves that almost all the particles were sedimented to the bottom. Other lines represent different concentrations of protein solution; with increased protein concentration, the absorbance decreased less rapidly. The highest protein concentration (4% solid dark blue line) has the slowest reduction of absorbance, and the lowest protein concentration (0.5% solid green line) is the closest to the control. From the pictures of the resuspended HA pellets, it could be seen that the turbidity of the suspension increases with increased protein concentration.

From the absorbance graphs, it is observed that at lower protein concentrations, the reduction speed for WPI is lower than that in SC, which means the suspension stability was better acted for WPI at lower protein concentrations. When it reached the fully covered concentration, SC-coated HA presented a slightly higher absorbance value than WPI-coated HA powders, specifically, improved suspension stability for SC if the protein concentration was higher. This could additionally be noticed from the resuspension photo; more particles are suspended in higher protein concentrations for SC compared to WPI.

Figure 16 provides the absorbance graph for Capolac. A variance in the control group was observed in the diagram. Both SC and WPI illustrated a slower reduction in absorbance for pure Capolac particles resuspended in water within the time range. After 50 minutes, the absorbance value still remained around half of the original value; compared to pure HA particles, the absorbance value dropped to less than 20% of the initial value.

For other samples, Capolac displayed a comparable trend for HA. With increased protein concentration, the reduction in absorbance was shrunk more slowly. The highest absorbance was found in the highest protein concentration sample, and vice versa. Also, for lower protein concentrations, WPI has demonstrated a better performance than SC. For higher protein concentrations, the absorbance ended in a higher value for SC than WPI.

Some deviations could be found in the graph, especially for lower WPI concentration samples; they intersect with the control group. This could be due to experimental factors, such as sampling errors or instrument malfunction. Or it could be the reason that if lower concentrations of whey protein were added, there would be no significant improvement of the suspension stability for the Capolac particles.

(A)

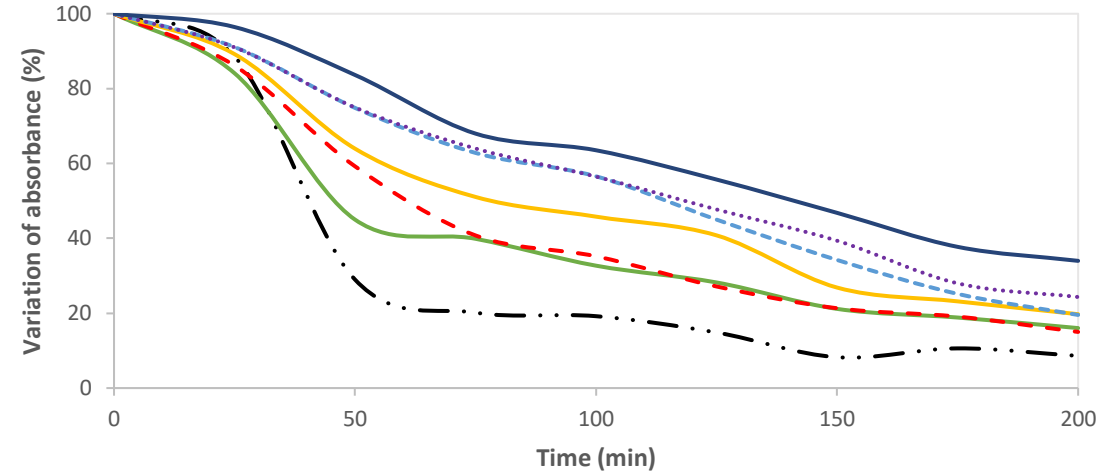

(B)

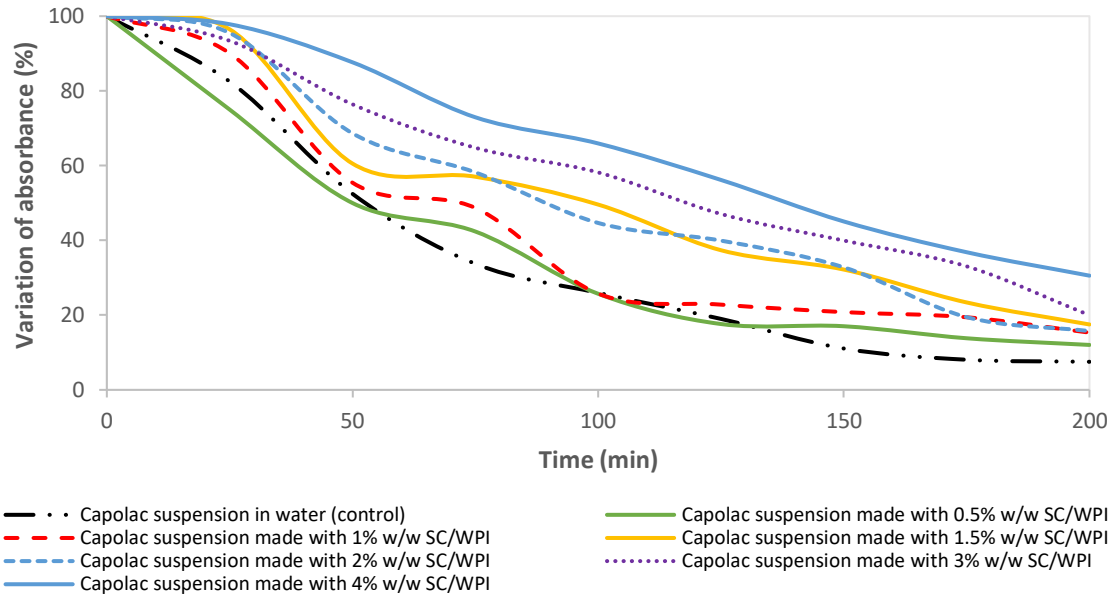

Figure 16. Absorbance as a function of time of suspension of CA particles (0.125% w/w) made with different concentrations of SC/WPI solutions. (A) SC; (B) WPI.

The photographs of the resuspended Capolac pellets in Milli-Q water after 24 hours with no disturbance are shown below; see figure 17.

(A) (B)

Figure 17. Suspension photos of the Capolac pellets in water: (A) CA with SC; (B) CA with WPI. From left to right, the protein concentration increased. The first one on the left is the control group without adding protein.

The suspension photos of Capolac pellets have further proved that the control sample is more turbid than the control in HA pellets, suggesting better suspension stability for the pure Capolac particles. When the Capolac pellets were resuspended in the same concentration as HA pellets (10%), like WPI, the particles were all suspended. Therefore the resuspended concentration was lower to 3% in order to better observe the difference; like SC, with higher protein concentrations, more particles were suspended.

To associate with the results from SDS-PAGE, these resuspension photos are in accordance with the gel images. A distinct color was diminishing for the bands in the SC gel image, indicating an improved adsorption for the particles onto proteins. For WPI, a less distinct color gradients were observed, but with higher protein concentration, the particles were still adsorbing to the protein. Like the photo, the higher concentration samples have more turbid suspensions.

Another turbidity measurement – the measurement of the reduction in scattered light through a turbidimeter is displayed in *Appendix 7* (figures A3-A4).

Figure A3 and A4 indicate that with increased protein concentrations (both SC and WPI), the suspension stability increased for both HA and Capolac particles. Overall speaking, the outcome from this method ends up in a higher turbidity value than the results of the spectrophotometer. The turbidity value decreased rapidly for pure HA after 50 minutes for both proteins, which are around 40% of the initial value compared to 10% in the spectrophotometer. With increased protein concentration, the turbidity value decreased more slowly along with time. The highest concentration matches the slowest decline degree of the turbidity value and vice versa.

For Capolac, it displays a roughly similar curve to HA particles, but generally higher turbidity value, with increased protein concentrations, the more gently the turbidity value reduced. With the lowest concentration of proteins, the more rapidly the reduction in turbidity value. However, it still has some details that differ from the HA, especially with the pure particles. In the original particle, which is the solid black line, the reduction in absorbance was much slower than in the pure HA particles. According to figure A4, even the pure Capolac particles showed good suspension stability compared to pure HA particles, and with added protein, the suspension stability improved furthermore.
The generally measured turbidity value was higher than the absorbance value from the spectrophotometer may be due to the different methods applied. For turbidity measurements,

the actual original measurement was shaken thoroughly and well mixed; then the later measurements were used with the same sample standing undisturbed after each time interval. But for the spectrophotometer, a disposable plastic cuvette was applied for each measurement. The samples could differ from each other depending on the sampling technique.

Anyhow, results from the different methods were consistent, and both proved that with increased protein concentration, the suspension stability would be enhanced for both HA and Capolac powders. And pure Capolac particles have a better suspension ability than pure HA particles.

4.7. Statistical analysis

4.7.1. Relationship between zeta-potential and the surface protein coverage

After measuring zeta-potential and calculating surface protein concentration, the relationship between the zeta-potential and the surface protein coverage of the powders was analyzed by Excel. A linear relationship was confirmed between the surface protein coverage and the zeta-potential for both HA and Capolac powders, see figure 18.

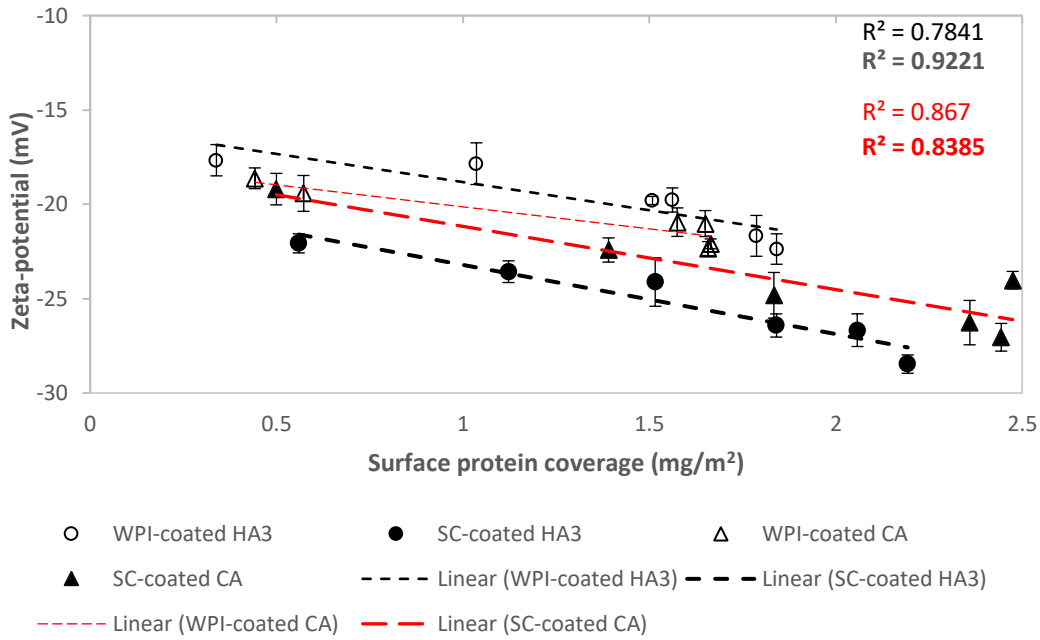

Figure 18. Linear relationship between the surface protein coverage of the protein-coated HA and Capolac particles and the zeta potential of the corresponding particles suspended in water.

According to previous zeta-potential and surface protein concentration results (see *sections 4.3, 4.5*), both zeta-potential and surface protein concentration for both HA and Capolac increase along with the increased protein concentration, and the threshold for both HA and Capolac is increased up to 2% of SC and 1.5% for WPI, implying a direct correlation between zeta-potential and the surface protein coverage. Therefore, a regression test was conducted, and, with the P value all less than 0.05, rejecting the null hypothesis of "no correlation", as a result, a linear relationship was confirmed for both HA and Capolac. Due to the aggressively increased absolute value of the zeta potential because of added protein, the zero point without added protein was excluded in the linear relationship. The summary of the regression statistics and the original separate linear relationship (including pure particles) is displayed in *Appendix 8*.

From Figure 18, both SC-coated particles and WPI-coated particles exhibited a linear relationship. The linear correlation for both SC and WPI-coated HA is both high, with values of R square up to 0.78 and 0.92, respectively. In the results of Capolac, it is no doubt that the linear relationships were confirmed between the surface protein coverage and zeta-potential for both SC-coated particles and WPI-coated particles. This indicates that with increased surface protein coverage, the absolute zeta potential value increases; in other words, the more stable the particle will be. From the original linear relationship for Capolac (figure A6 in *Appendix 8*), it can be known that Capolac exhibits an even stronger linear relationship with included zero protein concentration points. This could be due to the higher absolute value of zeta potential for pure Capolac particles, with added protein, the zeta potential was not drastically decreased, thus the linear correlation is much higher.

4.7.2. Adsorption modeling

Both Langmuir and Freundlich model were fitted with software R for both HA and Capolac. The acquired isotherm graphs are illustrated below; see figure 19. The original separate modeling for all the scenarios is presented in *Appendix 9*.

The parameters for the adsorption of SC and WPI on the two particles for both Langmuir and Freundlich models were calculated and obtained from the software R, see table 6.

Table 6. Isotherm parameters for Langmuir and Freundlich's models obtained by software R. q_m is the maximum monolayer surface coverage, K_L is the Langmuir affinity constant (100g/g), K_F is the Freundlich affinity constant ((100g/g)^N), n is the surface heterogeneity parameter, r^2 is the correlation coefficient.

Model	Parameters	HA - SC		HA - WPI		Capolac -SC		Capolac -WPI	
		value	S.E.	value	S.E.	value	S.E.	value	S.E.
Langmuir	q_m	3.37	0.29	2.77	0.51	3.74	0.74	2.67	0.82
	K_L	0.62	0.09	0.59	0.25	0.60	0.28	0.56	0.39
	r^2	0.99		0.95		0.94		0.88	
Freundlich	K_f	1.14	0.09	1.01	0.13	1.38	0.19	0.94	0.18
	n	1.91	0.28	1.99	0.51	2.02	0.55	1.97	0.70
	r^2	0.96		0.89		0.88		0.79	

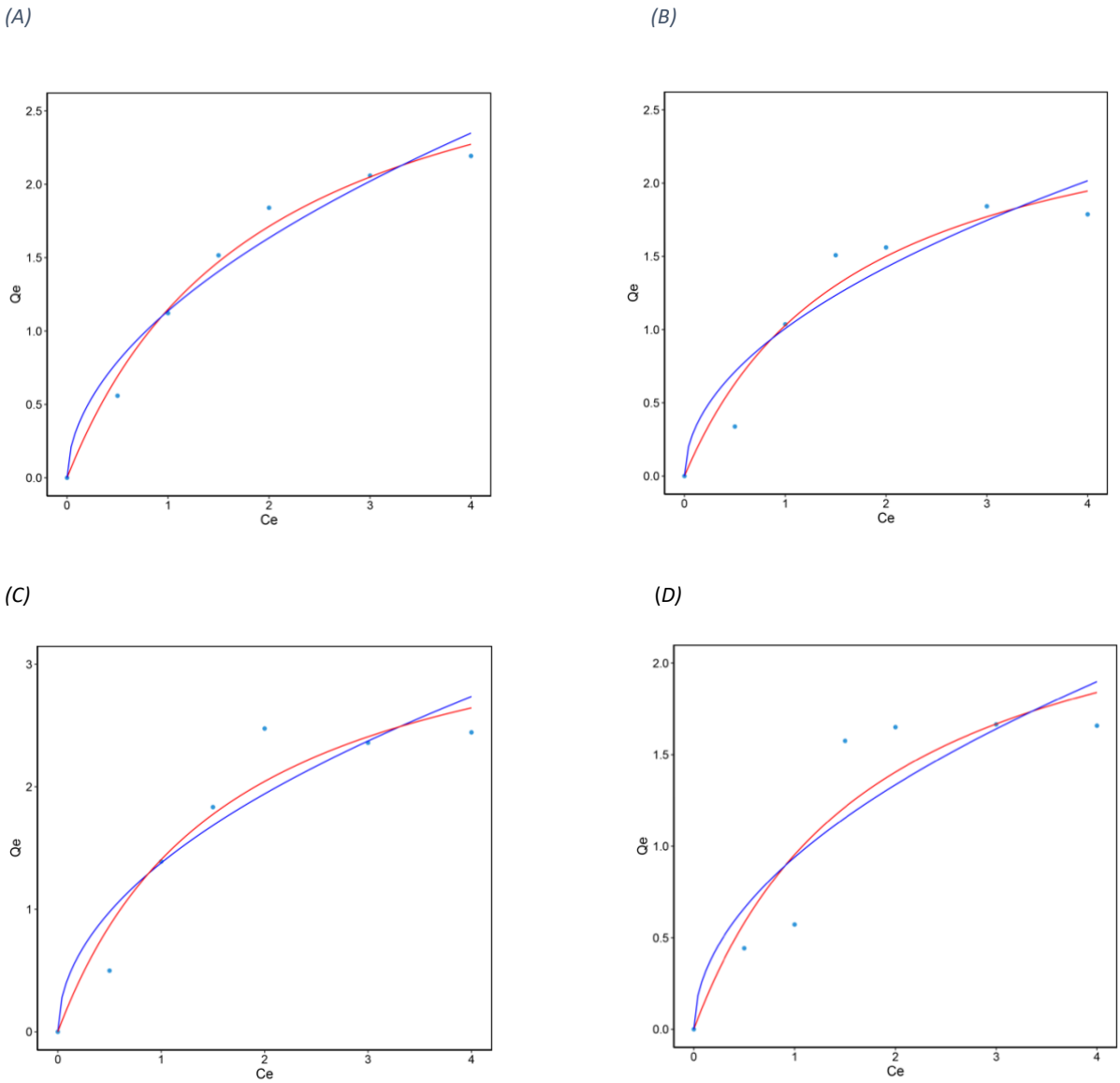

Figure 19. Isotherms of milk proteins adsorbed onto HA and Capolac, and the different model curves: (a) SC for HA particles; (b) WPI for HA particles; (c) SC for Capolac particles; (d) WPI for Capolac particles. The red line represents the Langmuir model, the blue line represents the Freundlich model. Ce represents the protein concentration at equilibrium (g/100g), Qe represents the surface protein concentration (mg/m^2).

As stated in figure 19, both models fit the experimental data for all 4 situations to some extent. However, if investigate carefully into the 8 curves, the red line (Langmuir model) fitted better for the experimental data, because the data came to a threshold and keeps the trend which is in accordance with the red curves. Unlike this trend, the blue line are continuously keeping upwards at the end of the curve, heading for a different direction.

From the parameters table (table 6), it is also obvious that the Langmuir is not only a favorable fitting, but also accurate modeling for the lab data. The correlation coefficients (r^2) for the four circumstances are all higher than those of the Freundlich model, suggesting that the Langmuir model is a better pattern, and the high correlation coefficient value denotes a very well-fitted model.

If we compare the affinity constant for SC and WPI in both models (k_l and k_f), the value is higher in SC than in WPI in all four scenarios, for example, 0.602 for Capolac-SC, higher than 0.557 for Capolac-WPI. This parameter expresses that the affinity of sodium caseinate for HA/Capolac is higher than whey protein's affinity to HA/Capolac. This finding is consistent with the previous results for SC and WPI respectively, in which the suspension stability is a little bit higher for SC than WPI.

Although some research showed that the Freundlich model fitted better for the adsorption of BSA on acid-functionalized HA than the Langmuir model mainly due to the proteins aggregating and forming multiple layers on the surface of HA, and possible interactions may happen between protein and the surface (Lee et al., 2012; Mavropoulos et al., 2011), the results from this lab data displayed a better fit pattern for Langmuir than the other one, indicating that the heterogeneity of the particle surface (HA/Capolac) may not affect the adsorption process. Anyhow, further investigations could be made to find the best-fitted model. No matter which model is adopted, the adsorption of the protein onto the surface of Capolac could be predicted and controlled.

To summarize, the different methods applied in this study clearly demonstrated that the protein adsorbed onto the surface of the HA/Capolac particles. With SC-coated or WPI-coated particles, the suspension stability of the Capolac can improve. The suspension ability of SC-coated particles exhibited better performance than WPI-coated particles.

Whey protein has an unfortunate record of inconsistent and unreliable physical functional performance in food systems, which may explain the results of the SDS-PAGE or the resuspension observations. Still, these could be solved through an expansion of the application, including nontraditional applications and the development of novel fractionation technologies (Smithers et al., 1996).

This project also revealed that the Capolac is a more stable particle than pure HA particles. The reason may depend on how Capolac is produced. As a by-product of cheese manufacturing, Capolac is a natural milk mineral concentrate that is high in natural calcium phosphate and other minerals, as well as protein concentrate. After the acid precipitation of the milk in the production process, a unique isolation process is applied to separate the mineral concentrate; during this process, some protein fractions with minerals are potentially left. Hence, the Capolac particles could be already coated partly by the protein fractions. According to the findings in this study, the partially covered particles decreased the zeta potential and enhanced the suspension stability.

5. Conclusion

The interactions between milk proteins and insoluble calcium salts have been poorly investigated. Because keeping the particles in the suspension as much as possible without adding external ingredients such as hydrocolloids is a big challenge. This study revealed that there are ways to improve the suspension stability of insoluble calcium salts, thereby promoting and supporting the research and development of calcium-fortified products.

Protein adsorption to a solid mineral surface is a complex phenomenon influenced by factors like protein properties, adsorbent properties, and environmental conditions. To be more specific, the protein size, surface properties of the protein and the adsorbent material, structure

of the protein, the concentration of protein, etc. are all factors that could affect the phenomenon (Barone et al., 2022).

The different particle size experimental scenarios proved that the adsorption ability would increase correspondingly with smaller particle sizes. In addition, the various measurements applied in this study proved that both SC and WPI adsorbed onto the HA and Capolac particles. SC-coated particles exhibited a better suspension stability than WPI-coated particles.

The surface structure of the absorbent (HA/Capolac) also plays a crucial role in the adsorption. The good correlation between the zeta-potential and surface protein load proved that the protein loading increased with higher surface charge density, which is determined by the relative ratio of calcium to phosphate or other salts on the adsorbent, and vice versa.

Capolac, a product developed in smaller particle size, meets one of the conditions that are beneficial to the suspension ability, it has also discovered a way to improve further its suspension stability. The protein-coated insoluble particles have increased negative zeta potential value and demonstrated enhanced colloidal stability when suspended in water. This was further verified by modeling, which also provided a way to predict the adsorption process.

To summarize, this study represents a promising beginning and offers a fresh concept to enhance Capolac's performance. However, before the utilization and implementation of this protein-coated product, certain aspects and trials may need to be further explored later on.

6. Future works

As stated in the conclusion part, protein adsorption to a solid mineral surface is a complicated phenomenon affected by multiple factors. Some of them still lack investigations.

For example, the insoluble salts' sensory defects like chalkiness and grittiness could also mitigate with reduced particle size. This sensory evaluation could be conducted in subsequent pilot trials.

Besides, the microstructure of the particles, for example, a smooth and crystalline microstructure, will end up in less protein binding compared to an irregularly shaped 3-D dimension structure. More investigations could be conducted to observe the microstructure of both HA and Capolac particles, as well as the adsorbed proteins, as it is highly relevant in predicting the particles' colloidal properties. Additionally, the differences in the conformations of the two adsorbed proteins may also reveal the deviations in the zeta-potential values for SC and WPI-coated particles could be due to the differences in charge density, or structure of the two protein molecules.

As previously mentioned, protein adsorption to a solid surface is a complex process affected by various environmental factors as well, like pH, temperature, processing technology, etc.; this project is just an investigation of one aspect under a stable, neutral pH environment. Conditions and stability may change under processing; thus, more trials or pilot experiments are required to move forward. The preference for adsorption on individual proteins could also be further explored by analyzing software on the SDS-PAGE gel results. This could help to fully understand the surface composition of the Capolac particles covered by casein and whey proteins.

This improved suspension stability of calcium salts, like Capolac, will not only broaden the application in calcium-fortified products but also have the potential to upgrade the calcium bioavailability in the products due to the higher calcium homogeneity in the product.

References

Amjad, Z. (2013). *Calcium phosphates in biological and industrial systems*. Springer Science & Business Media.

Barone, G., O'Regan, J., Kelly, A. L., & O'Mahony, J. A. (2022). Interactions between whey proteins and calcium salts and implications for the formulation of dairy protein-based nutritional beverage products: A review. *Comprehensive Reviews in Food Science and Food Safety*, *21*(2), 1254-1274.

Bee, S.-L., & Hamid, Z. A. (2020). Hydroxyapatite derived from food industry bio-wastes: Syntheses, properties and its potential multifunctional applications. *Ceramics International*, *46*(11), 17149-17175.

Bischoff, K. M., Shi, L., & Kennelly, P. J. (1998). The detection of enzyme activity following sodium dodecyl sulfate–polyacrylamide gel electrophoresis. *Analytical biochemistry*, *260*(1), 1-17.

Calvo, M., Kumar, R., & HEATH III, H. (1988). Elevated secretion and action of serum parathyroid hormone in young adults consuming high phosphorus, low calcium diets assembled from common foods. *The Journal of Clinical Endocrinology & Metabolism*, *66*(4), 823-829.

Calvo, M. S., Kumar, R., & HEATH III, H. (1990). Persistently elevated parathyroid hormone secretion and action in young women after four weeks of ingesting high phosphorus, low calcium diets. *The Journal of Clinical Endocrinology & Metabolism*, *70*(5), 1334-1340.

Cashman, K. D. (2006). Milk minerals (including trace elements) and bone health. *International Dairy Journal*, *16*(11), 1389-1398. https://doi.org/https://doi.org/10.1016/j.idairyj.2006.06.017

Chen, X. (2015). Modeling of experimental adsorption isotherm data. *information*, *6*(1), 14-22.

Clark, F. (1958). Dietary Levels of Families in the United States1. *Journal of the American Dietetic Association*, *34*(4), 378-382. https://doi.org/https://doi.org/10.1016/S0002-8223(21)17115-9

Clogston, J. D., & Patri, A. K. (2011). Zeta potential measurement. In *Characterization of nanoparticles intended for drug delivery* (pp. 63-70). Springer.

Cormick, G., Betran, A. P., Romero, I. B., Lombardo, C. F., Gulmezoglu, A. M., Ciapponi, A., & Belizan, J. M. (2019). Global inequities in dietary calcium intake during pregnancy: a systematic review and meta-analysis. *BJOG*, *126*(4), 444-456. https://doi.org/10.1111/1471-0528.15512

Crudden, A., Afoufa-Bastien, D., Fox, P. F., Brisson, G., & Kelly, A. L. (2005). Effect of hydrolysis of casein by plasmin on the heat stability of milk. *International Dairy Journal*, *15*(10), 1017-1025.

de Zawadzki, A., & Skibsted, L. H. (2019). Increasing calcium solubility from whey mineral residues by combining gluconate and δ-gluconolactone. *International Dairy Journal*, *99*, 104538.

DeKruif, C., & Holt, C. (2003). Advanced Dairy Chemistry, Vol. 1: Proteins, PF Fox and PLH McSweeney, editors. In: Kluwer Academic/Plenum Publishers, New York.

Dickinson, E. (1994). Protein-stabilized emulsions. In *Water in foods* (pp. 59-74). Elsevier.

Dickinson, E. (1997). Properties of emulsions stabilized with milk proteins: overview of some recent developments. *Journal of Dairy Science*, *80*(10), 2607-2619.

Fardet, A., Dupont, D., Rioux, L.-E., & Turgeon, S. L. (2019). Influence of food structure on dairy protein, lipid and calcium bioavailability: A narrative review of evidence. *Critical Reviews in Food Science and Nutrition*, *59*(13), 1987-2010.

Fox, P. F., Mcsweeney, P. L., & Paul, L. (1998). Dairy chemistry and biochemistry.

Freundlich, H. (1906). Over the adsorption in solution. *J. Phys. chem*, *57*(385471), 1100-1107.

Gallardo, V., Morales, M., Ruiz, M., & Delgado, A. (2005). An experimental investigation of the stability of ethylcellulose latex: correlation between zeta potential and sedimentation. *European journal of pharmaceutical sciences*, *26*(2), 170-175.

Gaucheron, F. (2005). The minerals of milk. *Reproduction Nutrition Development*, *45*(4), 473-483.

Gbassi, G., Yolou, F., Sarr, S., Atheba, P., Amin, C., & Ake, M. (2012). Whey proteins analysis in aqueous medium and in artificial gastric and intestinal fluids. *International Journal of Biological and Chemical Sciences*, *6*(4), 1828-1837.

Gorbunoff, M. J., & Timasheff, S. N. (1984). The interaction of proteins with hydroxyapatite: III. Mechanism. *Analytical biochemistry*, *136*(2), 440-445.

Hashim, M. A., Nadtochii, L. A., Muradova, M. B., Proskura, A. V., Alsaleem, K. A., & Hammam, A. R. (2021). Non-Fat Yogurt Fortified with Whey Protein Isolate: Physicochemical, Rheological, and Microstructural Properties. *Foods*, *10*(8), 1762.

Huang, F., Wang, Z., Zhang, J., Du, W., Su, C., Jiang, H., Jia, X., Ouyang, Y., Wang, Y., Li, L., Zhang, B., & Wang, H. (2018). Dietary calcium intake and food sources among Chinese adults in CNTCS. *PLoS One*, *13*(10), e0205045. https://doi.org/10.1371/journal.pone.0205045

Hulmi, J. J., Lockwood, C. M., & Stout, J. R. (2010). Effect of protein/essential amino acids and resistance training on skeletal muscle hypertrophy: A case for whey protein. *Nutrition & metabolism*, *7*(1), 1-11.

Iafisco, M., Di Foggia, M., Bonora, S., Prat, M., & Roveri, N. (2011). Adsorption and spectroscopic characterization of lactoferrin on hydroxyapatite nanocrystals. *Dalton Transactions*, *40*(4), 820-827.

Jeewanthi, R. K. C., Lee, N.-K., & Paik, H.-D. (2015). Improved functional characteristics of whey protein hydrolysates in food industry. *Korean journal for food science of animal resources*, *35*(3), 350.

Joint, F. (2004). *Vitamin and mineral requirements in human nutrition*. Diamond Pocket Books (P) Ltd.

Juriaanse, A., Booij, M., Arends, J., & Ten Bosch, J. (1981). The adsorption in vitro of purified salivary proteins on bovine dental enamel. *Archives of Oral Biology*, *26*(2), 91-96.

Lancker, J. L. V. (1976). Calcium and Phosphorus Metabolism. In *Molecular and Cellular Mechanisms in Disease* (pp. 331-359). Springer.

Langmuir, I. (1916). The constitution and fundamental properties of solids and liquids. Part I. Solids. *Journal of the American chemical society*, *38*(11), 2221-2295.

Lee, W.-H., Loo, C.-Y., Van, K. L., Zavgorodniy, A. V., & Rohanizadeh, R. (2012). Modulating protein adsorption onto hydroxyapatite particles using different amino acid treatments. *Journal of The Royal Society Interface*, *9*(70), 918-927.

Lewis, M. J. (2011). The measurement and significance of ionic calcium in milk–a review. *International Journal of Dairy Technology*, *64*(1), 1-13.

Ma, X., & Chatterton, D. E. (2021). Strategies to improve the physical stability of sodium caseinate stabilized emulsions: A literature review. *Food Hydrocolloids*, *119*, 106853.

Mavropoulos, E., Costa, A. M., Costa, L. T., Achete, C. A., Mello, A., Granjeiro, J. M., & Rossi, A. M. (2011). Adsorption and bioactivity studies of albumin onto hydroxyapatite surface. *Colloids and surfaces B: Biointerfaces*, *83*(1), 1-9.

McKenzie, H. (1967). Milk proteins. *Advances in Protein Chemistry*, *22*, 55-234.

Mehta, R. (2022). Nutritional interventions of osteoporosis.

Mura-Galelli, M., Voegel, J., Behr, S., Bres, E., & Schaaf, P. (1991). Adsorption/desorption of human serum albumin on hydroxyapatite: a critical analysis of the Langmuir model. *Proceedings of the National Academy of Sciences*, *88*(13), 5557-5561.

Nakanishi, K., Sakiyama, T., & Imamura, K. (2001). On the adsorption of proteins on solid surfaces, a common but very complicated phenomenon. *Journal of bioscience and bioengineering*, *91*(3), 233-244.

Nayak, A. K. (2010). Hydroxyapatite synthesis methodologies: an overview. *International Journal of ChemTech Research*, *2*(2), 903-907.

Neville, J., Armstrong, K., & Price, J. (2001). Ultra Whey 99: a whey protein isolate case study. *International Journal of Dairy Technology*, *54*(4), 127-129.

Omoarukhe, E. D., ON‐NOM, N., Grandison, A. S., & Lewis, M. J. (2010). Effects of different calcium salts on properties of milk related to heat stability. *International Journal of Dairy Technology*, *63*(4), 504-511.

Onwulata, C., & Huth, P. (2009). *Whey processing, functionality and health benefits* (Vol. 82). John Wiley & Sons.

Organization, W. H. (2004). *Vitamin and mineral requirements in human nutrition*. World Health Organization.

Palacios, C., Hofmeyr, G. J., Cormick, G., Garcia-Casal, M. N., Pena-Rosas, J. P., & Betran, A. P. (2021). Current calcium fortification experiences: a review. *Ann N Y Acad Sci*, *1484*(1), 55-73. https://doi.org/10.1111/nyas.14481

Patel, A. R., Bouwens, E. C., & Velikov, K. P. (2010). Sodium caseinate stabilized zein colloidal particles. *Journal of Agricultural and Food Chemistry*, *58*(23), 12497-12503.

Patel, S. (2015). Functional food relevance of whey protein: A review of recent findings and scopes ahead. *Journal of Functional Foods*, *19*, 308-319.

Pawal, A. D. (2019). Calcium Deficiency in Women. *Think India Journal*, *22*(13), 686-690.

Pitkowski, A., Durand, D., & Nicolai, T. (2008). Structure and dynamical mechanical properties of suspensions of sodium caseinate. *Journal of Colloid and Interface Science*, *326*(1), 96-102.

Portale, A., Halloran, B., Murphy, M., & Morris, R. C. (1986). Oral intake of phosphorus can determine the serum concentration of 1, 25-dihydroxyvitamin D by determining its production rate in humans. *The Journal of clinical investigation*, *77*(1), 7-12.

Ross, A. C. (2011). The 2011 report on dietary reference intakes for calcium and vitamin D. *Public Health Nutr*, *14*(5), 938-939. https://doi.org/10.1017/S1368980011000565

Rouahi, M., Champion, E., Gallet, O., Jada, A., & Anselme, K. (2006). Physico-chemical characteristics and protein adsorption potential of hydroxyapatite particles: influence on in vitro biocompatibility of ceramics after sintering. *Colloids and surfaces B: Biointerfaces*, *47*(1), 10-19.

Salopek, B., Krasic, D., & Filipovic, S. (1992). Measurement and application of zeta-potential. *Rudarsko-geolosko-naftni zbornik*, *4*(1), 147.

Sharpe, J., Sammons, R., & Marquis, P. (1997). Effect of pH on protein adsorption to hydroxyapatite and tricalcium phosphate ceramics. *Biomaterials*, *18*(6), 471-476.

Simonne, A., Simonne, E., Eitenmiller, R., Mills, H., & Cresman Iii, C. (1997). Could the Dumas method replace the Kjeldahl digestion for nitrogen and crude protein determinations in foods? *Journal of the Science of Food and Agriculture*, *73*(1), 39-45.

Singh, G., Arora, S., Sharma, G., Sindhu, J., Kansal, V., & Sangwan, R. (2007). Heat stability and calcium bioavailability of calcium-fortified milk. *LWT-Food Science and Technology*, *40*(4), 625-631.

Smithers, G., Ballard, F., Copeland, A., De Silva, K., Dionysius, D., Francis, G., Goddard, C., Grieve, P., Mcintosh, G., & Mitchell, I. (1996). Symposium: advances in dairy foods processing and engineering. *Journal of Dairy Science*, *79*, 1454-1459.

Sousa, G. T., Lira, F. S., Rosa, J. C., de Oliveira, E. P., Oyama, L. M., Santos, R. V., & Pimentel, G. D. (2012). Dietary whey protein lessens several risk factors for metabolic diseases: a review. *Lipids in health and disease*, *11*(1), 1-9.

Tercinier, L. (2016). Study of the interactions between milk proteins and hydroxyapatite particles [Ph.D. thesis.]. *Massey University, Riddet Institute, Palmerston North, New Zealand.*

Tercinier, L., Ye, A., Anema, S., Singh, A., & Singh, H. (2013). Adsorption of milk proteins on to calcium phosphate particles. *Journal of Colloid and Interface Science*, *394*, 458-466.

Theobald, H. E. (2005). Dietary calcium and health. *Nutrition Bulletin*, *30*(3), 237-277.

Tsakali, E., Petrotos, K., D'Allessandro, A., & Goulas, P. (2010). A review on whey composition and the methods used for its utilization for food and pharmaceutical products. Proc. 6th Int. Conf. Simul. Modelling Food Bioind,

Tuinier, R., & De Kruif, C. (2002). Stability of casein micelles in milk. *The Journal of chemical physics*, *117*(3), 1290-1295.

Tunick, M. H. (1987). Calcium in Dairy Products. *Journal of Dairy Science*, *70*(11), 2429-2438. https://doi.org/https://doi.org/10.3168/jds.S0022-0302(87)80305-3

Vigneshkumar, P., George, E., Joseph, J., John, F., & George, J. (2022). Liposomal bionanomaterials for nucleic acid delivery. In *Fundamentals of Bionanomaterials* (pp. 327-362). Elsevier.

Walstra, P. (1990). On the stability of casein micelles. *Journal of Dairy Science*, *73*(8), 1965-1979.

Walstra, P., Walstra, P., Wouters, J. T., & Geurts, T. J. (2005). *Dairy science and technology*. CRC press.

Weaver, C. M. (1998). Calcium in food fortification strategies. *International Dairy Journal*, *8*(5-6), 443-449. https://doi.org/10.1016/s0958-6946(98)00067-3

Ye, A. (2008). Interfacial composition and stability of emulsions made with mixtures of commercial sodium caseinate and whey protein concentrate. *Food Chemistry*, *110*(4), 946-952.

Appendix

Appendix 1. Product sheet of Capolac from Arla Food Ingredients.

Arla Foods Ingredients
Discovering the wonders of whey

Capolac® MM-0525 BG

PRODUCT DESCRIPTION:

Capolac® MM-0525 BG is a natural milk mineral concentrate derived from milk, with a high content of calcium. Capolac® MM-0525 BG is designed for easily fortifying a wide range of food and beverage products with the benefits of calcium from a natural source.

INDUSTRY:

- Health Foods
- Medical Nutrition
- Early Life Nutrition
- Dairy

APPLICATION:

- Ready-to-mix powder
- Clear RTD
- Protein Bars
- Tablets

PROPERTIES:

- Natural milk minerals
- High in calcium content, in a similar form to the calcium composition of teeth and bone
- High in phosphorus

CHEMICAL SPECIFICATIONS	Unit	Specification Min.	Specification Max.	Typical value	Frequency of analysis	Analytical method
Protein as is (Na6.38)	%		3.0		Each batch	ISO 8968-3 / IDF 20-3
Lactose	%	6.0	10.0		Each batch	ISO 5765-2
Fat	%		1.0		Each batch	ISO 1736/IDF 9
Ash	%	70.0	78.0		Each batch	ISO 5545 /IDF 90
Moisture*	%		5		Each batch	NIR
Nitrate (NO3-)	ppm		100		Each batch	ISO 14673-3

* As measured after production.

MINERALS	Unit	Specification Min.	Specification Max.	Typical value	Frequency of analysis	Analytical method
Sodium (Na)	%			0.6	Monitoring	ICP
Magnesium (Mg)	%			0.7	Monitoring	ICP
Phosphorus (P)	%	11.0	15.0		Each batch	ICP
Chloride (Cl)	%			0.5	Monitoring	NMKL 178
Potassium (K)	%			0.6	Monitoring	ICP
Calcium (Ca)	%	24.0	29.0		Each batch	ICP

PHYSICAL SPECIFICATIONS	Unit	Specification Min.	Specification Max.	Typical value	Frequency of analysis	Analytical method
pH	10% sol	6.5	7.5		Each batch	ISO 5546 / IDF 115
Scorched particles	Disc		A		Each batch	ADPI
Bulk density (625s)	g/cm3	0.4	0.7		Each batch	ISO 8967 / IDF 134
Particle size	99%	<15 µm			Each batch	Malvern
Appearance	Description	Free from lumps			Each batch	Sensory inspection
Colour	Description	White to cream			Each batch	Sensory inspection
Flavour/odour	Description	Light milky			Each batch	Sensory inspection

MICROBIOLOGICAL SPECIFICATIONS	Unit	Specification		Frequency of analysis	Analytical method
		n	Max.		
Total plate count (30 °C)	CFU/g	2	10,000	Each batch	ISO 4833-1
Enterobacteriaceae	CFU/g	1	10	Each batch	ISO 21528-2
Bacillus cereus	CFU/g	1	100	Each batch	NMKL no 189
Sulph. Red. Clostridia	CFU/g	1	50	Each batch	NMKL No. 56, 5. Ed.
Yeast & mould	CFU/g	1	100	Each batch	ISO 6611
		n	Absent in		
Staphylococcus aureus		1	1 g	Each batch	ISO 6888-3
Salmonella		1	250 g	Each batch	ISO 6579
Listeria Monocytogenes		1	25 g	Monitoring	ISO 11290

NUTRITIONAL VALUES		
VALUES PER 100 G PRODUCT		
Energy	174/41	kJ/kcal
Calories from fat	0.9	Kcal
Protein (Nx6.25)	1.6	g
Carbohydrate	8.4	g
- of which dietary fiber	n.a.	
- of which sugars	8.4	g
- of which added sugars	n.a.	
Fat	0.1	g
- of which saturated fat	0.1	g
- of which trans fat	n.a.	
Cholesterol	n.a.	
Salt	1.5	g
Sodium	600	mg
Vitamin D	n.a.	
Calcium	26.6	%
Potassium	0.6	%
Iron	n.a.	

EU Energy value is calculated according to Regulation (EU) No 1169/2011 of the European Parliament and of the Council of 25 October 2011 on the provision of food information to consumers.

ALLERGENS			
YES	NO	ALLERGENS	DESCRIPTION OF COMPONENTS
	•	Cereals containing gluten and products thereof	
	•	Crustaceans and products thereof	
	•	Eggs and products thereof	
	•	Fish and products thereof	
	•	Peanuts and products thereof	
	•	Soya beans products thereof	
•		Milk and products thereof (including lactose)	Bovine milk
	•	Nuts	
	•	(Tree) Nuts and products thereof	
	•	Celery and products thereof	
	•	Mustard and products thereof	
	•	Sesame seeds and products thereof	
	•	Sulphur dioxide and sulphites (>10 mg/kg)	
	•	Lupin and products thereof	
	•	Molluscs and products thereof	

STORAGE:
Store in closed bags under cool and dry conditions to prevent deterioration due to humidity and high temperatures.

SHELF LIFE:
36 months if kept under the prescribed storage conditions.

PACKAGING:
Paper bags with a polyethylene inner liner containing 20 kg net.

LEGAL REFERENCES:
The product is manufactured, packaged and labelled according to the relevant EU-regulations for food and food ingredients, and/or FAO/ WHO Codex Alimentarius where applicable. This includes that the milk/milk constituents used as raw material originate from healthy cows. The milk used in the production is included in monitoring programmes for undesirable substances as required by regulations or HACCP-based risk assessment. The production plant is approved by the competent authorities and included in the EU register of approved food establishments.

Products manufactured outside EU complies with relevant regulations in the country where the product is produced.

GMO POLICY:
Arla Foods Ingredients Group P/S's objective is to avoid genetically modified ingredients in our products. The requirements we have established for our suppliers ensure that only non-GMO raw materials are used during production of our products. Therefore, our products and the raw materials used do not contain, consist of or are produced from GMOs as defined in regulation (EC) No 1829/2003 and they do not contain ingredients produced from GMOs. Therefore, our products do not need labelling according to Regulation (EC) No 1829/2003 and 1830/2003.

For the definition of GMOs we refer to EU Directive 2001/18/EC.

Appendix 2. Raw data for protein solutions and different suspensions.

Table A1. Raw data for both SC and WPI solutions.

Protein	ID	% w/w	Protein	Weighed (g)	Milli-Q (ml)
SC	1S	0	0	0	100
	2S	0.5	0.5	0.5033	99.5
	3S	1	1	1.008	99
	4S	1.5	1.5	1.5009	98.5
	5S	2	2	2.0003	98
	6S	3	3	3.0022	97
	7S	4	4	4.0006	96
WPI	1W	0	0	0	100
	2W	0.5	0.5	0.5008	99.5
	3W	1	1	1.0001	99
	4W	1.5	1.5	1.5019	98.5
	5W	2	2	2.0026	98
	6W	3	3	3.0009	97
	7W	4	4	4.0081	96

Table A2. Raw data for the supernatants and HA pellets for HA3 and the parameters for calculation of surface protein coverage.

				mdryssed	msup	mwetsed	pi	SA	Psup	mi	nitrogen content
Protein	ID	% w/w	Protein % w/w (9g)	HA (1g)	supernatant	HA pellets					
SC	SH1	0	Add 9ml 0% SC	1.0033	7.85556	0.4721	0	80	0	9.0084	0
	SH2	0.5	Add 9ml 0,5% SC	0.9929	7.7362	0.8361	0.5	80	0	9.0516	0
	SH3	1	Add 9ml 1% SC	1.0008	7.8113	1.1662	1	80	0	9.0082	0.000
	SH4	1.5	Add 9ml 1.5% SC	1.0029	7.7196	1.1676	1.5	80	0.15312	9.0396	0.024
	SH5	2	Add 9ml 2% SC	0.9998	7.7641	1.2911	2	80	0.39556	9.0209	0.062
	SH6	3	Add 9ml 3% SC	1.0065	7.6821	1.3202	3	80	1.26962	9.0069	0.199
	SH7	4	Add 9ml 4% SC	1.001	7.7106	1.0873	4	80	2.27766	9.087	0.357
WPI	WH1	0	Add 9ml 0% WPI	1.0019	7.8293	0.4663	0	80	0	9.0269	0
	WH2	0.5	Add 9ml 0,5% WPI	1.0106	8.4142	0.9197	0.5	80	0.24244	9.0496	0.038
	WH3	1	Add 9ml 1% WPI	1.0076	7.8982	1.2003	1	80	0.08932	9.0458	0.014
	WH4	1.5	Add 9ml 1.5% WPI	1.0038	8.2717	0.7672	1.5	80	0.18502	8.9386	0.029
	WH5	2	Add 9ml 2%WPI	1.0082	8.2301	0.8108	2	80	0.68904	9.0108	0.108

	WH6	3	Add 9ml 3% WPI	1.0015	8.6256	0.6705	3	80	1.52482	9.0079	0.239
	WH7	4	Add 9ml 4% WPI	1.0017	8.3762	0.7868	4	80	2.82634	9.0406	0.443

Table A3. Raw data for the supernatants and Capolac pellets for Capolac and the parameters for calculation of surface protein coverage.

				Mdryse d	msup	mwet sed	pi	SA	Psu p	mi	nitrogen content
Protein	ID	% w/w	Protein % w/w (9g)	HA (1g)	supernatant	CA pellets					
SC	SH1	0	Add 9ml 0% SC	1.0055	8.1922	1.0326	0	80	0	9.0553	0
	SH2	0.5	Add 9ml 0,5% SC	1.0028	8.0768	1.0005	0.5	80	0.1595	9.0838	0.025
	SH3	1	Add 9ml 1% SC	1.0052	8.0828	1.06	1	80	0	9.0852	0.000
	SH4	1.5	Add 9ml 1.5% SC	1.002	8.0016	1.0939	1.5	80	0.20416	9.0667	0.032
	SH5	2	Add 9ml 2% SC	1.0056	8.0986	0.9831	2	80	0.24882	9.0927	0.039
	SH6	3	Add 9ml 3% SC	1.0029	7.9876	0.9635	3	80	1.47378	9.0311	0.231
	SH7	4	Add 9ml 4% SC	1.0088	7.9352	1.0843	4	80	2.53286	9.0789	0.397
WPI	WH1	0	Add 9ml 0% WPI	1.004	8.1356	1.1141	0	80	0	9.021	0
	WH2	0.5	Add 9ml 0,5% WPI	1.0015	8.1294	1.1536	0.5	80	0.19778	9.0253	0.031
	WH3	1	Add 9ml 1% WPI	1.0033	8.1488	1.2196	1	80	0.63162	9.0149	0.099
	WH4	1.5	Add 9ml 1.5% WPI	1.0019	8.1247	1.3421	1.5	80	0.38918	9.0351	0.061
	WH5	2	Add 9ml 2%WPI	1.0075	8.1751	1.2041	2	80	0.8613	9.0087	0.135
	WH6	3	Add 9ml 3% WPI	1.0038	8.1106	1.1705	3	80	1.98418	9.0949	0.311
	WH7	4	Add 9ml 4% WPI	1.0116	8.1646	1.1382	4	80	3.0305	9.0064	0.475

Appendix 3. Original zeta-potential data of different HA particles for SC and WPI.

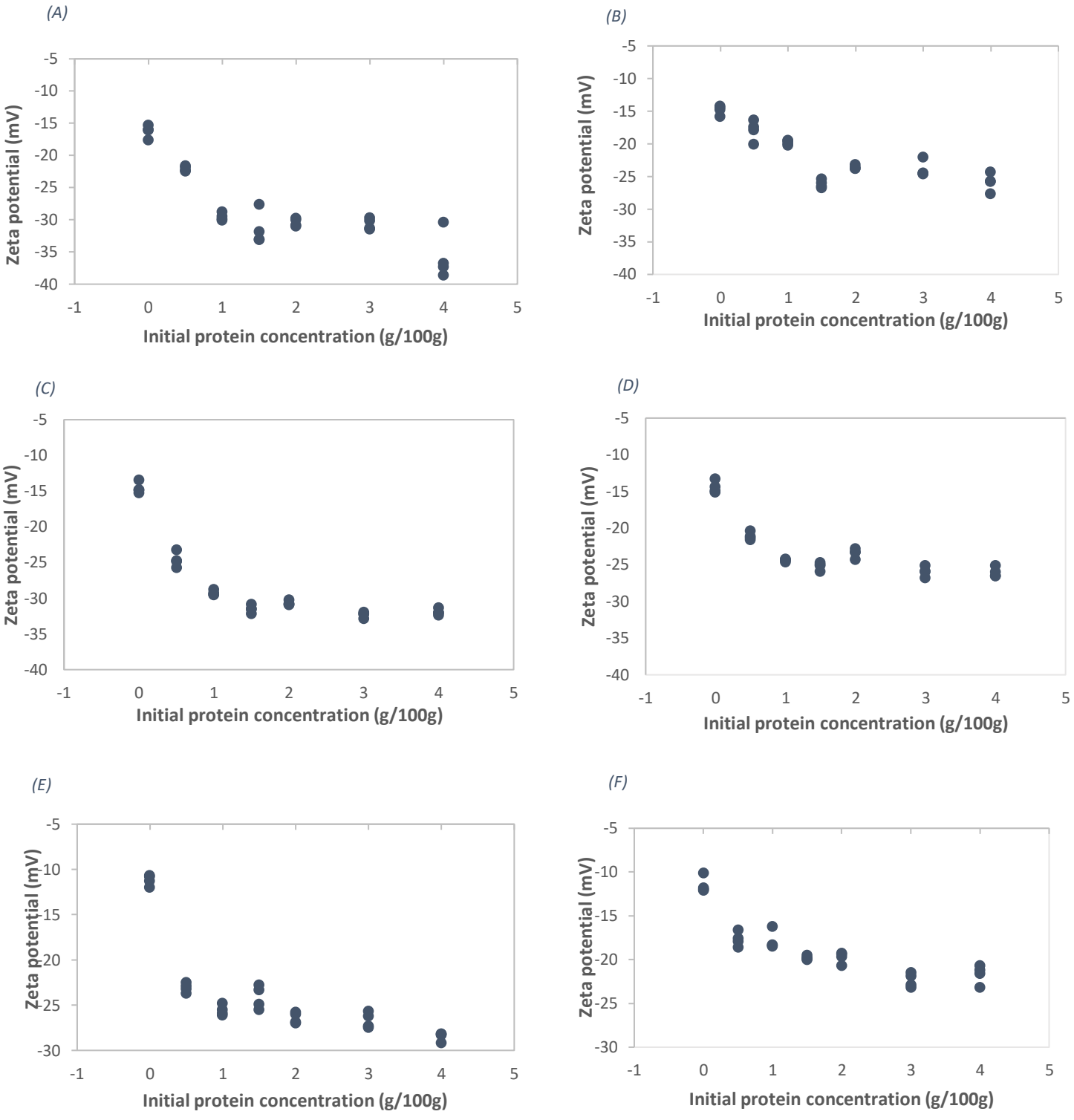

Figure A1. Zeta-potential of the three different batches of HA powders for both SC and WPI: (A) HA1 with SC; (B) HA1 with WPI; (C) HA2 with SC; (D) HA2 with WPI; (E) HA3 with SC; (F) HA3 with WPI.

Appendix 4. Summary of ANOVA test and Tukey test for zeta-potential of different HA particles.

Table A4. The different HA particles suspended in SC solution.

Data (average of 4 measurements):

Protein Concentration	HA1	HA2	HA3
0	-16.25	-14.65	-11.2
0.5	-22.075	-24.7	-23.075
1	-29.575	-29.3	-25.575
1.5	-31.425	-31.55	-24.125
2	-30.425	-30.75	-26.425
3	-30.675	-32.35	-26.675
4	-35.775	-31.966667	-28.475

Anova: Two-Factor Without Replication

SUMMARY	*Count*	*Sum*	*Average*	*Variance*
concentration0	3	-42.1	-14.033333	6.66083333
c0.5	3	-69.85	-23.283333	1.75520833
c1	3	-84.45	-28.15	4.991875
c1.5	3	-87.1	-29.033333	18.0727083
c2	3	-87.6	-29.2	5.801875
c3	3	-89.7	-29.9	8.501875
c4	3	-96.216667	-32.072222	13.3308565
HA1	7	-196.2	-28.028571	43.476756
HA2	7	-195.26667	-27.895238	40.9246032
HA3	7	-165.55	-23.65	33.2327083

ANOVA

Source of Variation	*SS*	*df*	*MS*	*F*	*P-value*	*F crit*
Rows	674.40127	6	112.400212	42.9512067	2.0097E-07	2.99612038
Columns	86.827328	2	43.413664	16.5895529	0.00035112	3.88529383
Error	31.4031349	12	2.61692791			
Total	792.631733	20				

Table A5. The different HA particles suspended in WPI solution.

Data (average of 4 measurements):

Protein Concentration	HA1	HA2	HA3
0	-14.875	-14.425	-11.5
0.5	-17.975	-21.1	-17.675
1	-19.85	-21.1	-17.675
1.5	-26.2	-24.375	-17.85
2	-23.6	-23.425	-19.775
3	-23.975	-25.925	-22.375
4	-25.925	-26.333333	-21.675

Anova: Two-Factor Without Replication

SUMMARY	*Count*	*Sum*	*Average*	*Variance*
concentration0	3	-40.8	-13.6	3.358125
c0.5	3	-56.75	-18.916667	3.59770833
c1	3	-58.625	-19.541667	3.00395833
c1.5	3	-68.425	-22.808333	19.2714583
c2	3	-66.8	-22.266667	4.66395833
c3	3	-72.275	-24.091667	3.16083333
c4	3	-73.933333	-24.644444	6.65488426
HA1	7	-152.4	-21.771429	18.454881
HA2	7	-156.68333	-22.383333	16.6377778
HA3	7	-128.525	-18.360714	12.8949702

ANOVA

Source of Variation	*SS*	*df*	*MS*	*F*	*P-value*	*F crit*
Rows	266.277937	6	44.3796561	24.6008812	4.4273E-06	2.99612038
Columns	65.7740146	2	32.8870073	18.2301854	0.00023055	3.88529383
Error	21.6478373	12	1.80398644			
Total	353.699788	20				

Table A6. The parameters applied in the Turkey test, obtained from the ANOVA summary table. k indicates sample number, n.obv is number of observations, Q is obtained from a reference table and a parameter to calculate the critical value.

	SC	WPI
k	3	3
n.obv	7	7
df	12	12
ms	2.61692791	1.80398644
combination	3	3
Q	3.77	3.77

Table A7. The summary for Turkey test for both SC and WPI.

	SC		
Comparison	Absolute difference	Critical value	Result
HA1-HA2	0.13333333	2.30509171	No
HA1-HA3	4.37857143	2.30509171	Yes
HA2-HA3	4.2452381	2.30509171	Yes
	WPI		
Comparison	Absolute difference	Critical value	Result
HA1-HA2	0.61190476	1.91385471	No
HA1-HA3	3.41071429	1.91385471	Yes
HA2-HA3	*4.022619048*	1.91385471	Yes

Appendix 5. Zeta potential original graphs for HA3 and CA powders.

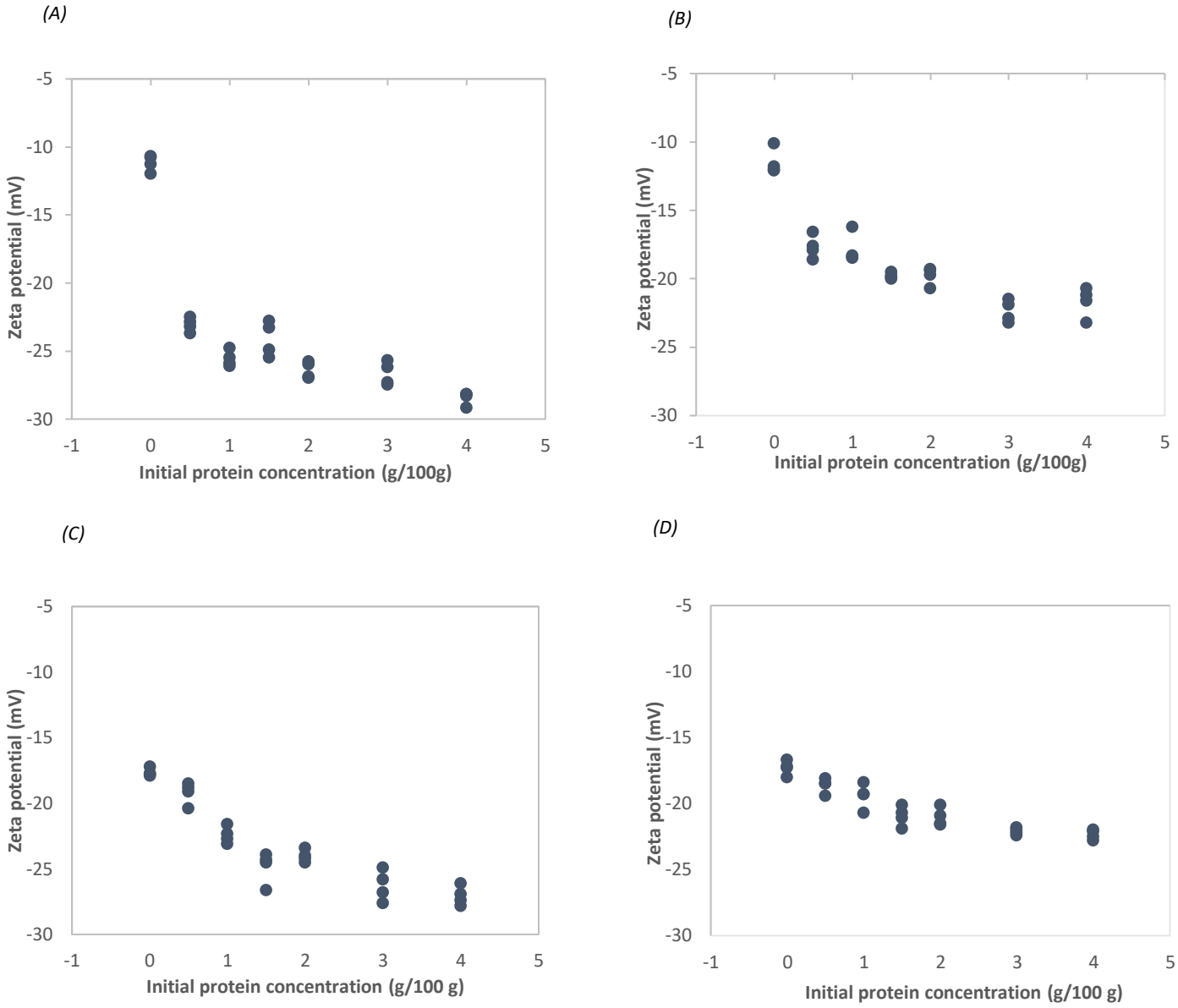

Figure A2. Effect of protein concentration on the zeta-potential of HA and Capolac particles that were suspended in SC or WPI solutions of different initial concentrations stirred for 2h and centrifuged, and the pellets were then resuspended in water. (A): HA3 suspended in SC; (B) HA3 suspended in WPI; (C) CA suspended in SC; (D) CA suspended in WPI.

Appendix 6. Average data and summary table for the ANOVA test of zeta-potential measurements for both HA and Capolac in SC and WPI.

Table A8. Average data for the zeta-potential in SC for both HA3 and CA and the summary table of the Anova test.

Data (average of 4 measurements):

Protein Concentration	HA3	CA
0	-11.2	-17.65
0.5	-23.075	-19.2
1	-25.575	-22.425
1.5	-24.125	-24.825
2	-26.425	-24.025
3	-26.675	-26.275
4	-28.475	-27.05

Anova: Two-Factor Without Replication

SUMMARY	*Count*	*Sum*	*Average*	*Variance*
0	2	-28.85	-14.425	20.80125
0.5	2	-42.275	-21.1375	7.5078125
1	2	-48	-24	4.96125
1.5	2	-48.95	-24.475	0.245
2	2	-50.45	-25.225	2.88
3	2	-52.95	-26.475	0.08
4	2	-55.525	-27.7625	1.0153125
HA3	7	-165.55	-23.65	33.2327083
CA	7	-161.45	-23.064286	12.4789286

ANOVA

Source of Variation	*SS*	*df*	*MS*	*F*	*P-value*	*F crit*
Rows	237.979911	6	39.6633185	6.55774308	0.01881035	4.28386571
Columns	1.20071429	1	1.20071429	0.19852035	0.6715437	5.98737761
Error	36.2899107	6	6.04831845			
Total	275.470536	13				

Table A9. Average data for the zeta-potential in WPI for both HA3 and CA and the summary table of the ANOVA test.

Data (average of 4 measurements):

Protein Concentration	HA3	CA
0	-11.5	-17.3
0.5	-17.675	-18.625
1	-17.85	-19.425
1.5	-19.8	-20.95
2	-19.775	-21.025
3	-22.375	-22.1
4	-21.675	-22.35

Anova: Two-Factor Without Replication

SUMMARY	*Count*	*Sum*	*Average*	*Variance*
0	2	-28.8	-14.4	16.82
0.5	2	-36.3	-18.15	0.45125
1	2	-37.275	-18.6375	1.2403125
1.5	2	-40.75	-20.375	0.66125
2	2	-40.8	-20.4	0.78125
3	2	-44.475	-22.2375	0.0378125
4	2	-44.025	-22.0125	0.2278125
HA3	7	-130.65	-18.664286	13.0543452
CA	7	-141.775	-20.253571	3.49113095

ANOVA

Source of Variation	*SS*	*df*	*MS*	*F*	*P-value*	*F crit*
Rows	87.8935714	6	14.6489286	7.72399724	0.01259014	4.28386571
Columns	8.84040179	1	8.84040179	4.66131285	0.0741784	5.98737761
Error	11.3792857	6	1.89654762			
Total	108.113259	13				

Appendix 7. Turbidity measurements by turbidimeter, the reduction in scattered light graphs.

(A)

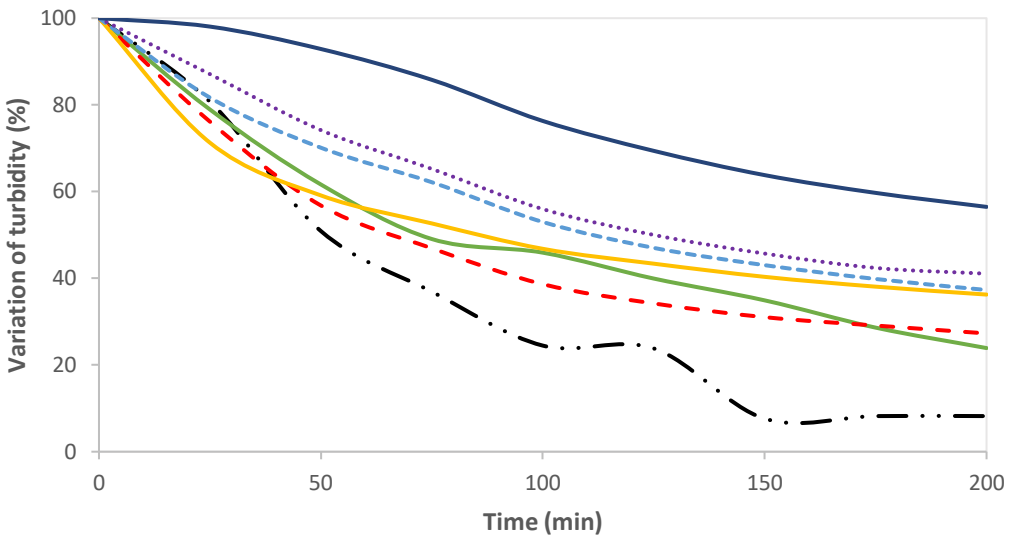

(B)

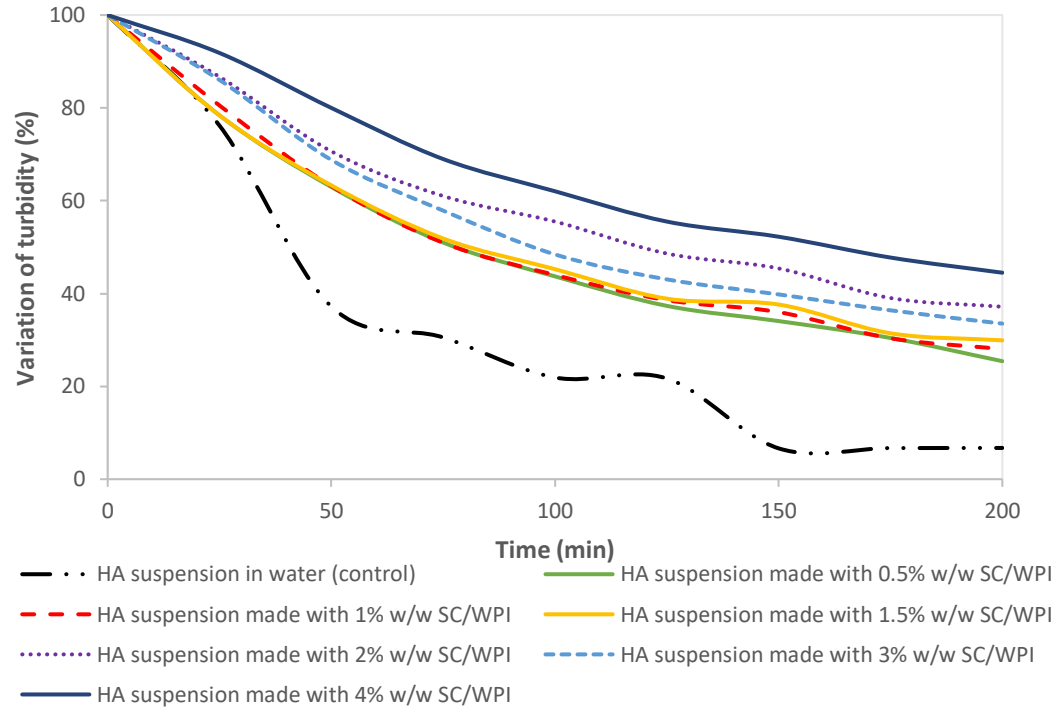

Figure A3. Turbidity as a function of time of suspension of HA3 particles (0.125% w/w) made with different concentrations of SC/WPI solutions. (A): HA3 with SC; (B) HA3 with WPI.

(A)

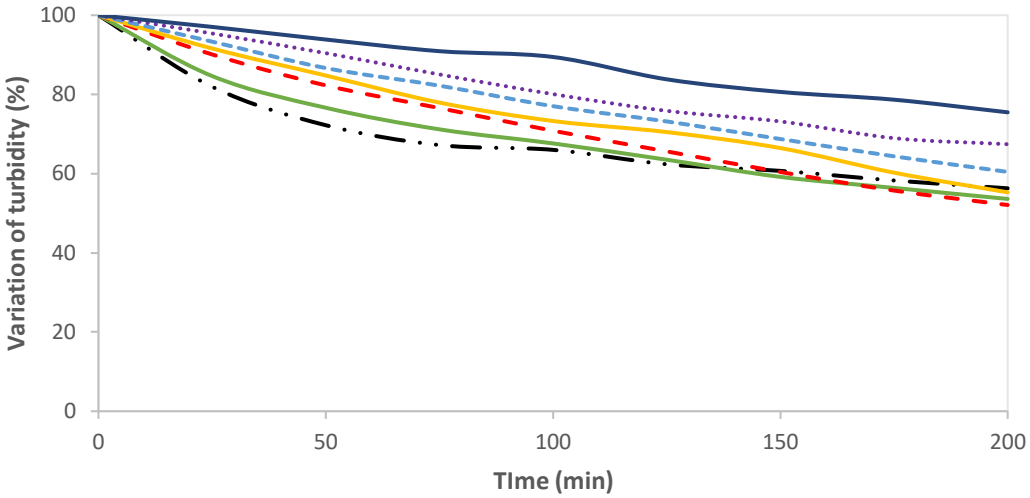

(B)

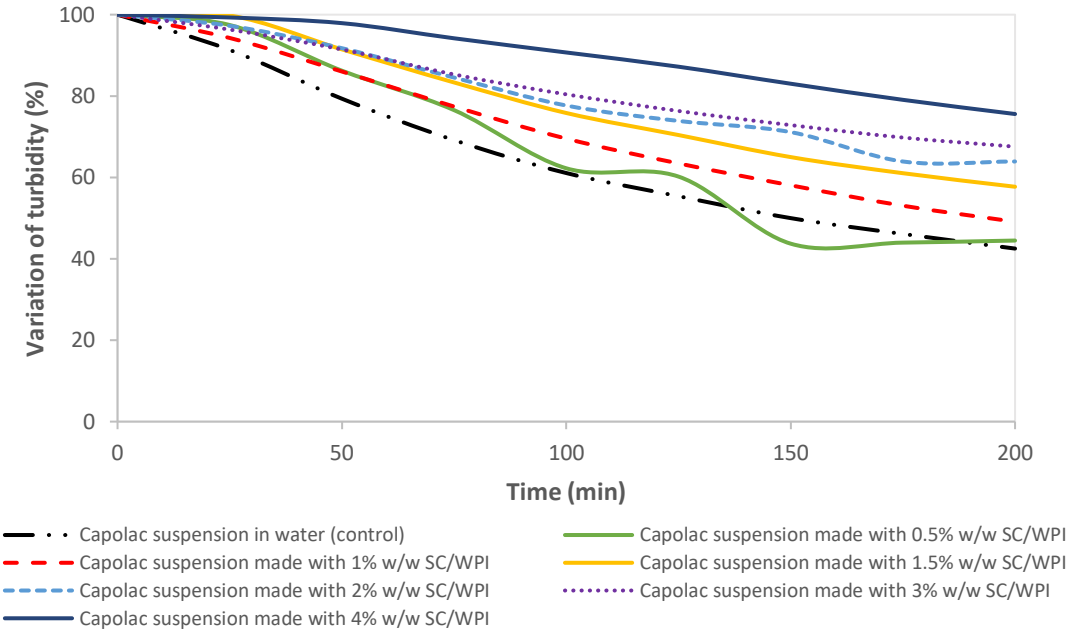

Figure A4. Turbidity as a function of time of suspension of Capolac particles (0.125% w/w) made with different concentrations of SC/WPI solutions. (A): CA with SC; (B) CA with WPI.

Appendix 8. The separate linear relationship with included zero points for both HA and Capolac, and the summary table of regression test for zeta potential and surface protein coverage for HA and Capolac.

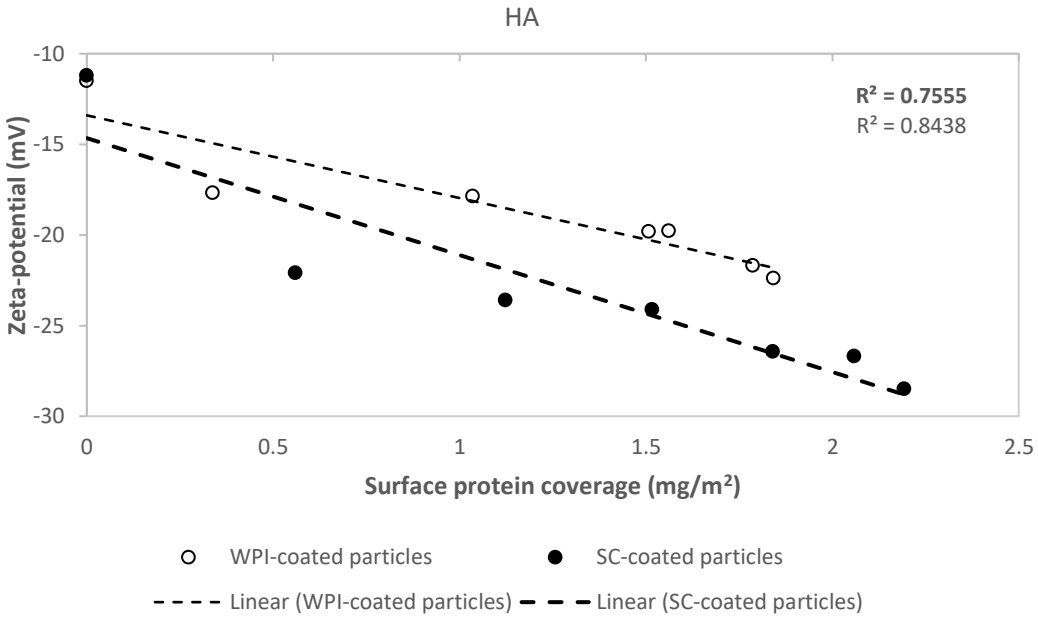

Figure A5. Linear relationship between the surface protein coverage of the protein-coated HA particles and the zeta potential of the corresponding particles suspended in water.

Table A10. Regression statistic for SC-coated HA.

Regression Statistics	
Multiple R	0.869187 39
R Square	0.755486 71
Adjusted R Square	0.706584 06
Standard Error	3.122660 16
Observations	7

ANOVA

	df	*SS*	*MS*	*F*	*Significance F*
Regression	1	150.641218	150.641218	15.44878 65	0.011064 81
Residual	5	48.75503 24	9.751006 48		
Total	6	199.39625			

	Coefficients	*Standard Error*	*t Stat*	*P-value*	*Lower 95%*	*Upper 95%*	*Lower 95.0%*	*Upper 95.0%*
Intercept	-15.481063	2.3900913	-6.4771835	0.00130737	-21.624985	-9.3371347	-21.624985	-9.3371347
X Variable 1	-6.1551385	1.56599599	-3.9304944	0.01106481	-10.180659	-2.1296177	-10.180659	-2.1296177

Table A11. Regression statistic for WPI-coated HA.

Regression Statistics	
Multiple R	0.91857636
R Square	0.84378252
Adjusted R Square	0.81253903
Standard Error	1.56450519
Observations	7

ANOVA

	df	*SS*	*MS*	*F*	*Significance F*
Regression	1	66.1035724	66.1035724	27.006662	0.00347631
Residual	5	12.2383825	2.4476765		
Total	6	78.3419549			

	Coefficients	*Standard Error*	*t Stat*	*P-value*	*Lower 95%*	*Upper 95%*	*Lower 95.0%*	*Upper 95.0%*
Intercept	-13.401579	1.17249759	-11.42941	8.9766E-05	-16.41558	-10.387578	-16.41558	-10.387578
X Variable 1	-4.5621097	0.87787013	-5.1967935	0.00347631	-6.8187467	-2.3054727	-6.8187467	-2.3054727

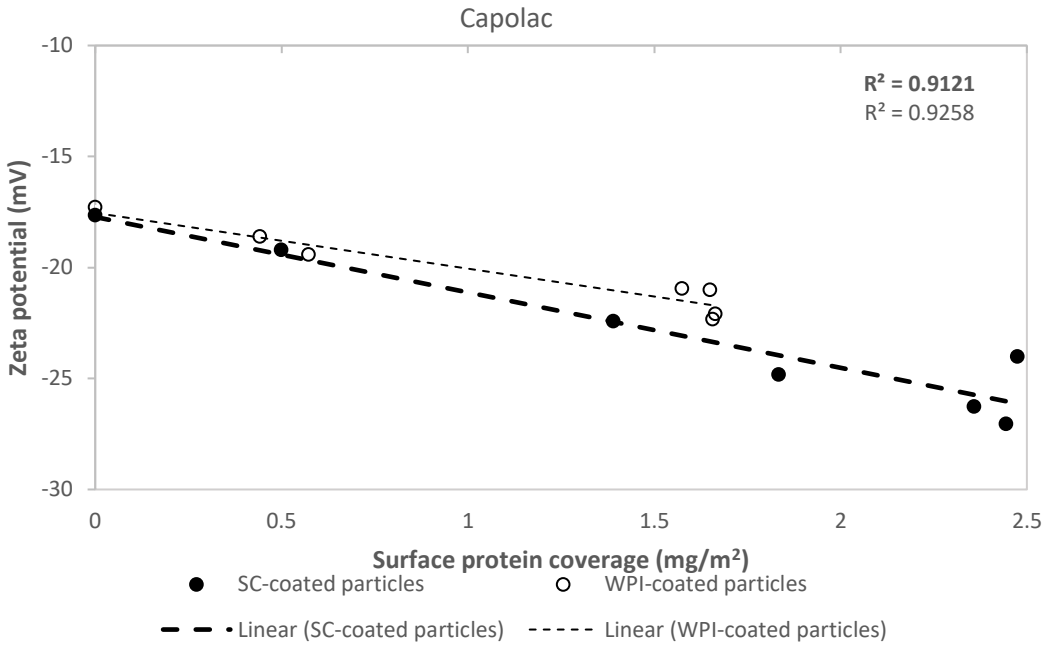

Figure A6. Linear relationship between the surface protein coverage of the protein-coated Capolac particles and the zeta potential of the corresponding particles suspended in water.

Table A12. Regression statistic for SC-coated Capolac.

Regression Statistics	
Multiple R	0.955045 71
R Square	0.912112 31
Adjusted R Square	0.894534 78
Standard Error	1.147210 96
Observations	7

ANOVA

	df	*SS*	*MS*	*F*	*Significance F*
Regression	1	68.293106 5	68.293106 5	51.890791 2	0.000803 23
Residual	5	6.5804649 5	1.3160929 9		
Total	6	74.873571 4			

	Coefficients	*Standard Error*	*t Stat*	*P-value*	*Lower 95%*	*Upper 95%*	*Lower 95.0%*	*Upper 95.0%*
Intercept	-17.725455	0.8586645	-20.643045	4.9383E-06	-19.932717	-15.518183	-19.932717	-15.518183
X Variable 1	-3.3967975	0.4715464 9	-7.2035263	0.0008032 3	-4.6089463	-2.1846487	-4.6089463	-2.1846487

Table A13. Regression statistic for WPI-coated Capolac

Regression Statistics	
Multiple R	0.96217475
R Square	0.92578025
Adjusted R Square	0.91093635
Standard Error	0.55761371
Observations	7

ANOVA

	df	*SS*	*MS*	*F*	*Significance F*
Regression	1	19.3921204	19.3921204	62.3675104	0.00052366
Residual	5	1.55466527	0.31093305		
Total	6	20.9467857			

	Coefficients	*Standard Error*	*t Stat*	*P-value*	*Lower 95%*	*Upper 95%*	*Lower 95.0%*	*Upper 95.0%*
Intercept	-17.542063	0.4028714	-43.542587	1.2058E-07	-18.577677	-16.506449	-18.577677	-16.506449
X Variable 1	-2.5102068	0.31785592	-7.8973103	0.0005236	-3.3272814	-1.6931322	-3.3272814	-1.6931322

Table A14. Regression statistic for SC-coated HA (without added protein).

Regression Statistics	
Multiple R	0.96024837
R Square	0.92207694
Adjusted R Square	0.90259617
Standard Error	0.73802588
Observations	6

ANOVA

	df	*SS*	*MS*	*F*	*Significance F*
Regression	1	25.7812712	25.781271 2	47.332684 8	0.00233888
Residual	4	2.17872883	0.5446822 1		
Total	5	27.96			

	Coefficients	*Standard Error*	*t Stat*	*P-value*	*Lower 95%*	*Upper 95%*	*Lower 95.0%*	*Upper 95.0%*
Intercept	-19.553008	0.87776377	-22.275934	2.4043E-05	-21.99007	-17.11594 5	-21.99007	-17.115945
X Variable 1	-3.6632029	0.53245194	-6.8798753	0.0023388 8	-5.1415265	-2.184879 4	-5.1415265	-2.1848794

Table A15. Regression statistic for WPI-coated HA (without added protein).

Regression Statistics	
Multiple R	0.88551183
R Square	0.7841312
Adjusted R Square	0.73016401
Standard Error	0.9986444
Observations	6

ANOVA

	df	*SS*	*MS*	*F*	*Significance F*
Regression	1	14.4904075	14.4904075	14.529774	0.01891098
Residual	4	3.98916253	0.99729063		
Total	5	18.47957			

	Coefficients	*Standard Error*	*t Stat*	*P-value*	*Lower 95%*	*Upper 95%*	*Lower 95.0%*	*Upper 95.0%*
Intercept	-15.83809	1.13041514	-14.010862	0.00015055	-18.976626	-12.699555	-18.976626	-12.699555
X Variable 1	-2.986842	0.78357917	-3.811794	0.01891098	-5.162407	-0.811279	-5.162407	-0.811279

Table A16. Regression statistic for SC-coated Capolac (without added protein).

Regression Statistics	
Multiple R	0.91571287
R Square	0.83853007
Adjusted R Square	0.79816258
Standard Error	1.2813587
Observations	6

ANOVA

	df	*SS*	*MS*	*F*	*Significance F*
Regression	1	34.1058129	34.1058129	20.772413	0.01035708
Residual	4	6.56752047	1.64188012		
Total	5	40.673333			

	Coefficients	*Standard Error*	*t Stat*	*P-value*	*Lower 95%*	*Upper 95%*	*Lower 95.0%*	*Upper 95.0%*
Intercept	-17.821564	1.44622004	-12.322858	0.00024916	-21.836914	-13.806213	-21.836914	-13.806213
X Variable 1	-3.3512395	0.73529563	-4.5576763	0.01035708	-5.3927474	-1.3097315	-5.3927474	-1.3097315

Table A17. Regression statistic for WPI-coated Capolac (without added protein).

Regression Statistics	
Multiple R	0.93113976
R Square	0.86702125
Adjusted R Square	0.83377657
Standard Error	0.59834859
Observations	6

ANOVA

	df	*SS*	*MS*	*F*	*Significance F*
Regression	1	9.33718668	9.33718668	26.0799945	0.00694934
Residual	4	1.43208415	0.35802104		
Total	5	10.7692708			

	Coefficients	*Standard Error*	*t Stat*	*P-value*	*Lower 95%*	*Upper 95%*	*Lower 95.0%*	*Upper 95.0%*
Intercept	-17.806402	0.62527469	-28.47727	9.0483E-06	-19.542443	-16.070361	-19.542443	-16.070361
X Variable 1	-2.3324646	0.45673187	-5.106857	0.00694934	-3.6005556	-1.0643736	-3.6005556	-1.0643736

Appendix 9. The original separate modeling isotherms, Langmuir and Freundlich modeling for both HA and Capolac of SC and WPI.

(A)

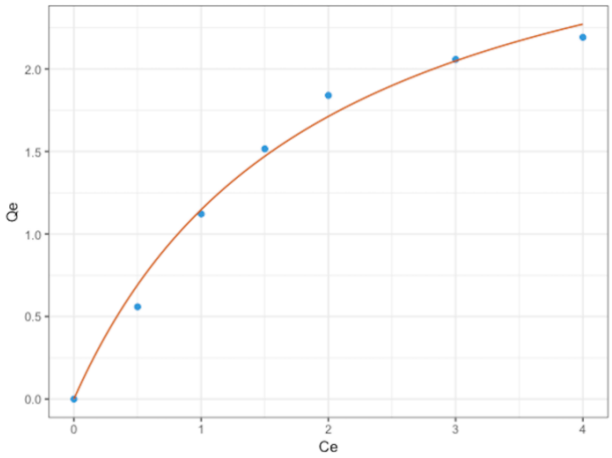

(B)

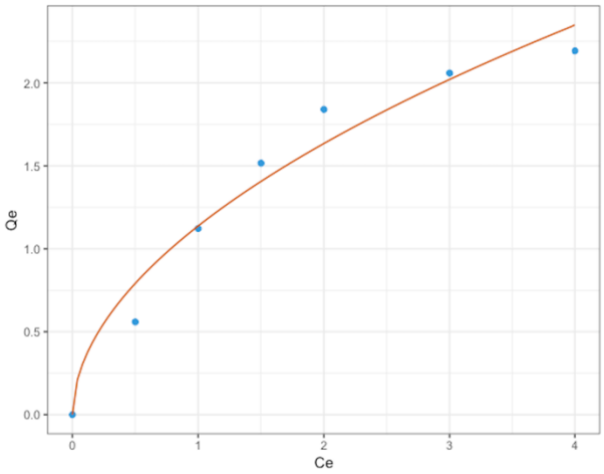

(C)

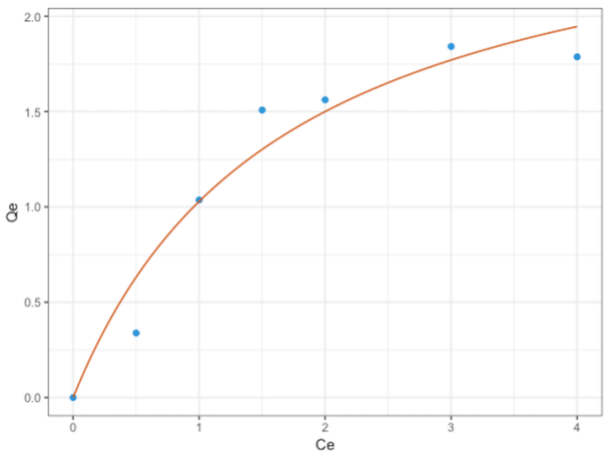

(D)

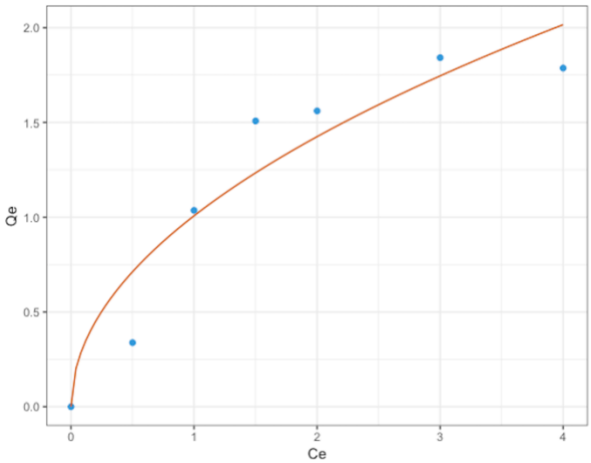

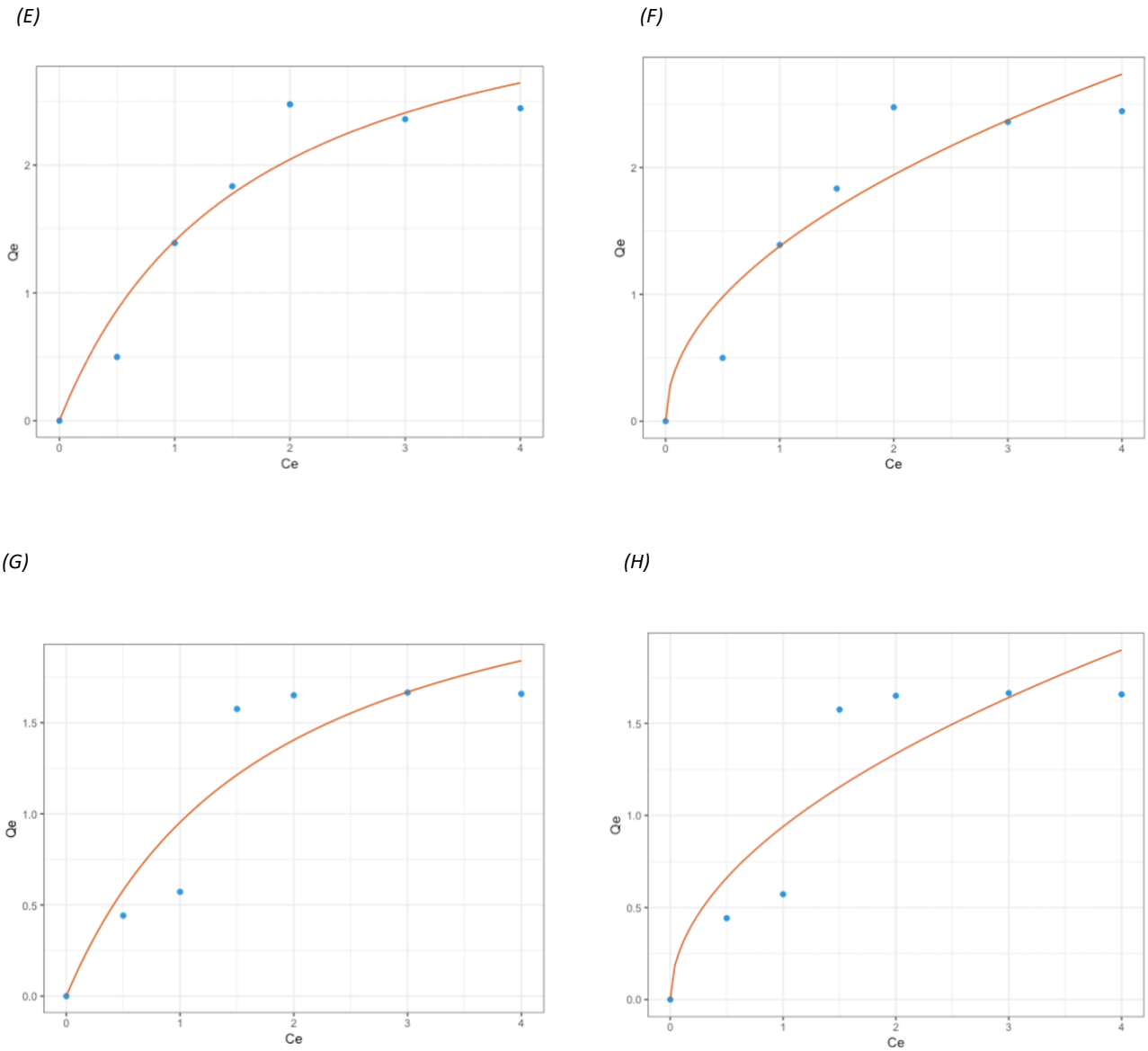

Figure A7. The original modeling isotherms obtained from software R: (A) Langmuir modeling for SC-coated HA; (B) Freundlich modeling for SC-coated HA; (C) Langmuir modeling for WPI-coated HA; (D) Freundlich modeling for WPI-coated HA; (E) Langmuir modeling for SC-coated Capolac; (F) Freundlich modeling for SC-coated Capolac; (G) Langmuir modeling for WPI-coated Capolac; (H) Freundlich modeling for WPI-coated Capolac.